

Non-equilibrium effects in steady relativistic $e^+e^-\gamma$ winds

Ole M. Grimsrud and Ira Wasserman

Center for Radiophysics and Space Research, Cornell University, Ithaca, New York 14853

ABSTRACT

We consider an ultra-relativistic wind consisting of electron-positron pairs and photons with the principal goal of finding the asymptotic Lorentz factor γ_∞ for zero baryon number. The wind is assumed to originate at radius r_i where it has a Lorentz factor γ_i and a temperature T_i sufficiently high to maintain pair equilibrium. As r increases, T decreases and becomes less than the temperature corresponding to the electron mass m_e , after which non-equilibrium effects become important. Further out in the flow the optical depth τ drops below one, but the pairs may still be accelerated by the photons until τ falls below $\sim 2 \times 10^{-5} \gamma_i^{3/4}$. Radiative transfer calculations show that only at this point do the radiation flux and pressure start to deviate significantly from their blackbody values. The acceleration of the pairs increases γ by a factor ~ 45 as compared to its value at the photosphere; it is shown to approach $\gamma_\infty \sim 1.4 \times 10^3 (r_i/10^6 \text{cm})^{1/4} \gamma_i^{3/4} T_i/m_e$.

The limit of zero baryon number is a good approximation when the mass injection rate \dot{M} in the flow is below a critical value corresponding to $(\dot{E}/\dot{M})_{c,0} \sim 5 \times 10^7 (r_i/10^6 \text{cm}) T_i/m_e$ for fixed energy injection rate \dot{E} . For large baryon loading, $\dot{E}/\dot{M} \lesssim (\dot{E}/\dot{M})_{c,M} \sim 350 (r_i/10^6 \text{cm})^{1/4} \gamma_i^{3/4} T_i/m_e$, the asymptotic Lorentz factor is $\gamma_\infty \sim \dot{E}/\dot{M}$. Surprisingly, increasing \dot{E}/\dot{M} from $(\dot{E}/\dot{M})_{c,M}$ to ∞ only increases γ_∞ by a factor $\sim (m_p/m_e)^{1/4} \approx 6.5$, less than an order of magnitude.

Subject headings: gamma rays: bursts – hydrodynamics – radiative transfer

1. Introduction

The release of a large amount of radiative energy into a small volume can lead to the formation of a fireball, a dense fluid of radiation and particles that expands under its own pressure. Fireball models have become the accepted framework for understanding gamma-ray bursts at cosmological distances and their afterglows (Paczynski 1986, 1990; Shemi & Piran 1990; Mészáros & Rees 1993, Piran 1997). Paczynski (1986) and Goodman (1986) originally considered the possibility that fireballs could originate in the collision of a pair of neutron stars in a binary star system coalescing as a result of gravitational radiation reaction. (See also Naryan, Paczynski & Piran 1992.) In this picture, the thermal energy released in the collision, $\sim 10^{53}$ ergs, is radiated as a neutrino-anti-neutrino burst. A fraction of that energy may be transformed into electron-positron

pairs above the surface of the neutron star (Goodman, Dar & Nussinov 1987). There are now additional proposals for the origin of fireballs (e.g. Paczyński 1997; Fuller & Shi 1997; Pen, Loeb & Turok 1997).

Close to the radius at which energy is injected, the resulting wind is opaque. The radiation energy that is initially trapped can escape in two different ways further out in the flow: When the plasma becomes optically thin, radiation streams freely to the observer (Paczyński 1990). Alternatively, if there is a significant baryon contamination in the fireball, it can become matter dominated before radiation escapes. The matter will increase the opacity and, more importantly, convert part of the radiation energy into bulk kinetic energy (Shemi & Piran 1990). Interactions between the expanding atmosphere and the surrounding matter provide a way to convert the kinetic energy in the baryons back to radiation at the resulting shock front (Mészáros & Rees 1993). Internal shocks due to variations in the velocity of matter is also proposed as a way to dissipate kinetic energy (Rees & Mészáros 1994). Fenimore (1997) recently pointed out that the observed temporal structure of gamma ray bursts severely constrains the proposed models of energy conversion by relativistic shocks; conceivably internal structure and shocks can account for some of the observed variability (e.g. Kobayashi, Piran & Sari 1997).

In the fireball models invoked to explain the afterglows of GRB 970228 and GRB 970508, the bulk Lorentz factor of the outflow is $\gamma \sim 100 - 1000$ before the outgoing shell is slowed significantly by sweeping up matter from ambient gas (Wijers, Rees & Mészáros 1997; Waxman 1997; Waxman, Kulkarni & Frail 1998). From a theoretical point of view, values of γ in this range yield acceptable estimates of burst duration and (with additional assumptions) characteristic photon energies. It is presumed that most of the energy originally in the fireball converts to kinetic energy long before deceleration begins, so the (baryon) rest mass of the flow must be nonzero: $\dot{M} = \dot{E}/\gamma$, where \dot{M} and \dot{E} are the rest mass and total energy injection rate of the flow. Precisely how such small but nonzero \dot{M}/\dot{E} arises is not clear yet; nor is it obvious whether $\gamma = \dot{E}/\dot{M}$ can be much larger or smaller than 100-1000, the values that seem necessary for modeling gamma ray bursts.

In this paper we reconsider the original steady wind problem first solved by Paczyński (1986) but for $\dot{M} \equiv 0$. At first sight, one might think that the result would be $\gamma \rightarrow \infty$. However, the failure of equilibrium at low temperatures (once the pair density falls sufficiently so that annihilation becomes slow) leads ultimately to a finite γ . As we shall see, in regions where the temperature is greater than the electron mass, the fireball is very optically thick because of the large number of electron–positron pairs. As the radius increases and the local temperature decreases, the deviation from equilibrium in the number density of pairs becomes significant. A little further out in the flow the optical depth falls below unity. However, the remaining pairs are still heated and accelerated considerably via their interactions with the radiation field; in the rest frame of the pairs, the radiation field itself remains close to the blackbody form long after the fireball becomes optically thin. The radiation spectrum detected by a stationary observer would not be blackbody, however, but also differs from the power-law spectra of GRBs. Although our calculations pertain to a steady, spherical wind, the general result that γ is finite even at

zero baryon mass may be true as well for thin shells emitted from impulsive energy release. We consider non-spherical perturbations around our wind solutions in Section 5.3; as we shall see, some memory of surface ‘hot-spots’ may persist out to the photosphere.

The dynamics for winds with sufficiently small baryon number are similar to $\dot{M} = 0$ outflow. A larger baryon number will increase the inertia of the flow, and so we expect the radiative acceleration and therefore the asymptotic Lorentz factor γ_∞ to be reduced. However, as the baryon number increases, the photospheric radius tends to increase as well, with a corresponding increase in the Lorentz factor at the photosphere. These two factors combined result in a surprisingly small variation in γ_∞ : For fixed \dot{E} , as \dot{E}/\dot{M} decreases from ∞ to $(\dot{E}/\dot{M})_{c,M} \sim 350(r_i/10^6 \text{ cm})^{1/4} \gamma_i^{3/4} T_i/m_e$, γ_∞ is only reduced by a factor of ~ 10 . For even smaller \dot{E}/\dot{M} , the baryons will dominate the energy of the flow even inside the photosphere, which results in a final Lorentz factor $\gamma_\infty \sim \dot{E}/\dot{M}$.

We present a detailed analytical model of the dynamics of the fireball in Section 3. This includes approximate results for the asymptotic value of the Lorentz factor and of the energy content in the pairs relative to that of the radiation, based on the initial temperature and initial velocity of the flow. Furthermore, we estimate where the pairs go out of equilibrium, the position of the photosphere, and the radius and optical depth at which the radiation fields start to deviate from their blackbody values. In Section 4 we show results from a numerical calculation to which the analytical model is compared. Next, based on the equation of radiative transfer, the comoving frame photon distribution function is shown to be very close to blackbody even out to quite small optical depths in these ultra-relativistic flows. The dynamical importance of baryons is described in Section 6. There we obtain approximate results in different regimes characterized by the amount of baryon loading, and we integrate the dynamical equations with baryons included in order to show how they affect the asymptotic Lorentz factor. Finally, we discuss qualitatively several possible extensions of our model, including the effects of (1) muon pairs and even nucleon pairs which could be present at sufficiently high temperatures; (2) a temperature anisotropy at the inner boundary, and (3) magnetic fields.

2. Equations

Consider a situation in which a large amount of energy is released into a compact region and the resulting relativistic outflow expands into vacuum. For simplicity we assume spherical symmetry and a stationary flow; gravity may also be neglected since we are interested in super-Eddington luminosities. (Perturbations away from exact spherical symmetry will be considered in Section 5.3.) The cross-sections for absorption and scattering, σ_a and σ_s , are taken to be constants; letting σ_a and σ_s cover a wide range of values in the numerical calculations facilitates a qualitative understanding of the effects of matter-radiation interactions. Throughout, units for which $k_B = \hbar = c = 1$ are used.

The temperature at the radius where energy is released is assumed to be high enough for pair creation to occur, and the flow is very optically thick close to its inner boundary. When the optical depth τ is $\gg 1$, the radiation field in the comoving frame will be close to blackbody. In a static or slowly expanding atmosphere one would expect the deviations from blackbody in the radiation field to be of order $1/\tau$. However, in an ultra-relativistic (Lorentz factor $\gamma \gg 1$) expanding atmosphere, the corrections to blackbody actually vanish to first order in $1/\tau$ and lowest order in $1/\gamma$. This will be discussed further in Section 7.

In the opposite limit, the optical depth approaches zero and the radiation streams freely. In this case a photon preserves its frequency in the lab frame as well as the quantity $(1 - \mu^2)r^2$, where μ is the direction cosine relative to the local radial direction. As the radial coordinate r gets large, the intensity therefore becomes increasingly sharply peaked in the outward radial direction; this is a purely geometrical effect (Hummer & Rybicki 1971). In a static or slowly moving atmosphere one would expect the radiation quantities to develop large deviations from their optically thick values soon after reaching the regime where $\tau < 1$. However, we shall find that in a rapidly expanding atmosphere the radiation field maintains its equilibrium form long after it decouples from the matter. This is similar to what happens in expanding universe cosmology, where the background radiation preserves its blackbody spectrum after decoupling. Specifically, as will be discussed in detail later (Section 3.4), we find that the radiation fields start deviating from blackbody radiation in the comoving frame only when $\tau \leq 2 \times 10^{-5} \gamma_i^{3/4}$.

This suggests a simple model for the radiation quantities: For $\tau > 1$, the radiation field is approximated as a blackbody distribution in the rest frame of the flow; for $\tau < 1$, the radiation energy, flux and pressure are given by the free-streaming approximation. We also need equations for the matter, characterized by its temperature T , Lorentz factor γ , and pair number density n_e . Energy and momentum conservation give two dynamical equations, whereas the Boltzmann equation determines the number density for the electrons and positrons.

2.1. Equations for $\tau > 1$

We assume that the flow originates at radius r_i where it has a Lorentz factor γ_i and temperature T_i . The basic equations describing the flow are found from the energy-momentum tensor,

$$T^{\alpha\beta} = \frac{2}{(2\pi)^3} \int p^\alpha p^\beta f \frac{d^3p}{E}. \quad (1)$$

p^α is the four-momentum, f the distribution function, and $E = \sqrt{p^2 + m^2}$ with m being the mass of the particle contributing to $T^{\alpha\beta}$. For the matter (e^\pm pairs for most of this paper)

$$T_M^{\alpha\beta} = (\rho_M + P_M)U^\alpha U^\beta + P_M g^{\alpha\beta}, \quad (2)$$

where ρ_M and P_M are the energy density and pressure measured in the rest frame of the flow and U^α is the matter four-velocity. We also need the following expressions for number density n ,

energy density ρ and pressure P :

$$n = \frac{2}{(2\pi)^3} \int f(p, T) 4\pi p^2 dp; \quad (3)$$

$$\rho = \frac{2}{(2\pi)^3} \int \sqrt{p^2 + m^2} f(p, T) 4\pi p^2 dp \quad \text{and} \quad (4)$$

$$P = \frac{1}{3} \frac{2}{(2\pi)^3} \int \frac{p^2}{\sqrt{p^2 + m^2}} f(p, T) 4\pi p^2 dp. \quad (5)$$

The non-zero components of the energy-momentum tensor for the radiation are $T_{\text{co}}^{00} = E_0, T_{\text{co}}^{01} = F_0, T_{\text{co}}^{11} = P_0$ and $T_{\text{co}}^{22} = T_{\text{co}}^{33} = (1/2)(E_0 - P_0)$ in the comoving frame, where the 1-direction is along the flow velocity; Lorentz transforming to an arbitrary reference frame gives

$$T_R^{00} = \gamma^2 [E_0 + 2vF_0 + v^2P_0] \quad (6)$$

$$T_R^{01} = \gamma^2 [v(E_0 + P_0) + (1 + v^2)F_0] = T_R^{10} \quad (7)$$

$$T_R^{11} = \gamma^2 [P_0 + 2vF_0 + v^2E_0] \quad (8)$$

$$T_R^{22} = \frac{1}{2}(E_0 - P_0) = T_R^{33}. \quad (9)$$

Below, we call E_0, P_0 and F_0 the (comoving frame) radiation energy density, pressure and flux (e.g. Mihalas & Mihalas 1984).

The equations describing the flow are given by $T_{;\beta}^{\alpha\beta} = 0$, where $T^{\alpha\beta} \equiv T_M^{\alpha\beta} + T_R^{\alpha\beta}$. With the assumptions of spherical symmetry and steady state, one gets

$$\frac{1}{r^2} \frac{d}{dr} \left\{ r^2 \left[(\rho_M + P_M + E_0 + P_0) \gamma \sqrt{\gamma^2 - 1} + (2\gamma^2 - 1)F_0 \right] \right\} = 0 \quad (10)$$

and

$$\frac{1}{r^2} \frac{d}{dr} \left\{ r^2 [(\rho_M + P_M + E_0 + P_0)(\gamma^2 - 1) + 2\gamma \sqrt{\gamma^2 - 1}F_0] \right\} + \frac{dP_M}{dr} + \frac{dP_0}{dr} + \frac{3P_0 - E_0}{r} = 0. \quad (11)$$

For large τ , the radiation has a blackbody distribution in the rest frame of the flow, and $E_0 = \pi^2 T^4/15, F_0 = 0$ and $P_0 = E_0/3$.

When the temperature in the rest frame of the fluid falls below m_e , the equilibrium $e^+ + e^- \rightleftharpoons 2\gamma$ can no longer be maintained. Consequently, the number densities of electrons and positrons will deviate from their equilibrium values and must be found from the Boltzmann equation,

$$\frac{p^\alpha}{m_e} \frac{\partial f}{\partial x^\alpha} = \left(\frac{\partial f}{\partial t} \right)_{\text{collisions}}. \quad (12)$$

Integrating over d^3p we get, in spherical symmetry,

$$\frac{1}{r^2} \frac{d}{dr} \left\{ r^2 n_e \gamma v \right\} = \left(\frac{\partial n_e}{\partial t} \right)_{\text{collisions}}. \quad (13)$$

For the process

$$e^- + e^+ \rightleftharpoons \gamma + \gamma', \quad (14)$$

the collision term is obtained by integrating the relevant matrix element times the factor $(f_\gamma f_{\gamma'} - f_- f_+)$ over phase space. Deviations from pair equilibrium become significant when T/m_e is small, so we may approximate $f_i \ll 1$ (i.e. $f_i = \exp[-(E_i - \mu_i)/T]$). We can therefore neglect Fermi suppression of electron and positron final states and stimulated emission of photons in the regions where equilibrium fails and the pair density ‘freezes out’. As will be seen later (Section 3.2), equilibrium is maintained until T is $\sim 0.05m_e$. With these approximations,

$$\left(\frac{\partial n_e}{\partial t}\right)_{\text{collisions}} = -\langle \sigma_{\text{ann}} v \rangle [n_e^2 - n_{e,\text{eq}}^2], \quad (15)$$

where $n_{e,\text{eq}}$ is the equilibrium number density of electrons; using this result, equation (13) can be written

$$\frac{1}{r^2} \frac{d}{dr} \{n_e r^2 \gamma v\} = -\langle \sigma_{\text{ann}} v \rangle [n_e^2 - n_{e,\text{eq}}^2]. \quad (16)$$

Svensson (1982) constructed a useful approximate expression for $\langle \sigma_{\text{ann}} v \rangle$, valid at all temperatures:

$$\langle \sigma_{\text{ann}} v \rangle = \frac{\pi r_e^2}{1 + 2(T/m_e)^2 / \ln [2\eta_E T/m_e + 1.3]} \quad (17)$$

Here r_e is the classical electron radius, $\eta_E \equiv \exp(-C_E)$ and $C_E \approx 0.5772$ is Euler’s constant. For the purpose of our analytical estimates we only need to know that $\langle \sigma_{\text{ann}} v \rangle \approx \pi r_e^2$ for $T \ll m_e$.

2.2. Equations for $\tau < 1$

For small τ , a good approximation to the radiation fields is found by assuming that photons stream freely from the photosphere to the observer. However, as the optical depth drops below one, energy and momentum may still be deposited by photons in the pair wind. Even though the energy and momentum deposition may be small compared to the energy-momentum content of the escaping photons, it may be large compared to that of the pairs. The dynamical equations must therefore take this interaction into account. We shall see that substantial acceleration of the e^\pm pairs occurs at $\tau < 1$.

The equation of radiative transfer can be written schematically as

$$k^\beta \frac{\partial}{\partial x^\beta} f_\gamma(k, x) = C_\gamma. \quad (18)$$

$f_\gamma(k, x)$ is the phase space distribution function of the photons, and the Lorentz invariant collision terms C_γ result from interactions with the electrons and positrons in the fluid.

We are interested in three processes: $e^\pm - \gamma$ scattering ($e^\pm + \gamma \rightarrow e^\pm + \gamma$), bremsstrahlung and its inverse ($e^\pm + e^\pm \rightleftharpoons e^\pm + e^\pm + \gamma$), and pair annihilation and creation ($e^+ + e^- \rightleftharpoons 2\gamma$). We

use a phenomenological model for the collision terms, evaluated in the rest frame of the flow. For scattering the collision term is

$$\mathcal{C}_s = 2n_e\sigma_s\tilde{k}^0 \left[-f_\gamma(k, x) + \int d^2\hat{n}' g(\hat{n}' \rightarrow \hat{n}) f_\gamma(k', x) \right] \quad (19)$$

where \tilde{k}^0 is the photon energy in the rest frame of the flow, and we assumed that the scattering is elastic ($\tilde{k}'^0 = \tilde{k}^0$). The probability distribution for direction changes in the rest frame is $g(\hat{n}' \rightarrow \hat{n})$. The cross section for scattering, σ_s , is taken to be a constant. The collision term for absorption and emission is

$$\mathcal{C}_a = 2n_e\sigma_a\tilde{k}^0 [-f_\gamma(k, x) + f_{\text{BB}}(\tilde{k}^0/T)], \quad (20)$$

where $f_{\text{BB}}(\tilde{k}^0/T)$ is the equilibrium photon distribution function at temperature T . The absorption cross section σ_a is also assumed to be constant.

Now take the first moment of the Boltzmann equation (18):

$$\frac{2}{(2\pi)^3} \int \frac{d^3k}{k^0} k^\alpha \left[k^\beta \frac{\partial}{\partial x^\beta} f_\gamma(k, x) \right] = \frac{2}{(2\pi)^3} \int \frac{d^3k}{k^0} k^\alpha C_\gamma. \quad (21)$$

We recognize the left hand side as $T_{R;\beta}^{\alpha\beta}$. The right hand side is the radiation force, which we denote G^α . The physical interpretation of the equations $T_{R;\beta}^{\alpha\beta} = G^\alpha$ (or $T_{M;\beta}^{\alpha\beta} = -G^\alpha$) is that $-G^0$ equals the net rate of radiative energy density input into the matter, while $-G^i$ is the net rate of radiative momentum input (Mihalas & Mihalas 1984). For the scattering term, taking the first moment over \mathcal{C}_s as indicated in equation (21) gives

$$G_{s,0}^0 = G_{s,0}^2 = G_{s,0}^3 = 0; \quad G_{s,0}^1 = -2n_e\sigma_s F_0, \quad (22)$$

where lower index 0 denotes that these quantities are evaluated in the comoving frame. The components of the radiation four-force corresponding to absorption and emission are

$$G_{a,0}^0 = -2n_e\sigma_a [E_0 - U_{\text{eq}}(T)] \quad G_{a,0}^1 = -2n_e\sigma_a F_0 \quad G_{a,0}^2 = G_{a,0}^3 = 0, \quad (23)$$

where $U_{\text{eq}}(T) = \pi^2 T^4/15$. Finally, for pair annihilation and creation we use the interpretations of G^α to write down directly

$$G_{p,0}^0 = 2m_e \langle \sigma_{\text{ann}} v \gamma \rangle [n_e^2 - n_{e,\text{eq}}^2(T)] \quad G_{p,0}^i = 0 \quad [i = 1, 2, 3]. \quad (24)$$

The energy loss of the plasma per annihilation is $(\gamma_- + \gamma_+)m_e$. Svensson (1982) gives an approximate expression for the pair annihilation cooling rate:

$$\langle \sigma_{\text{ann}} v \gamma \rangle = \frac{\pi r_e^2}{1/(1 + 6T/m_e) + (T/m_e) / \{ \ln [2\eta_E T/m_e + 1] + 1/4 \}}. \quad (25)$$

In the non-relativistic limit the energy loss is dominated by the rest mass energy, and one gets $\langle \sigma_{\text{ann}} v \gamma \rangle \approx \pi r_e^2$ for $T \ll m_e$.

Using the energy momentum tensor $T_M^{\alpha\beta}$ for the pairs and the components of the four force G^α as given above, the dynamical equations $T_{M;\beta}^{\alpha\beta} = -G^\alpha$ reduce to

$$(\rho_M + P_M) \frac{d \ln \gamma}{d \ln r} + \frac{d P_M}{d \ln r} = -\frac{r}{\gamma} G_0^r \quad (26)$$

and

$$\frac{d \rho_M}{d \ln r} + 2(\rho_M + P_M) + (\rho_M + P_M) \left(1 + \frac{1}{\gamma^2 - 1} \right) \frac{d \ln \gamma}{d \ln r} = -G_0^0 \frac{r}{\sqrt{\gamma^2 - 1}}. \quad (27)$$

Up to this point, no restriction to small optical depths has been invoked, and the dynamical equations can be applied at any τ , provided $f_\gamma(k, x)$ is determined. For $\tau < 1$, we assume that radiation streams outward freely. This is only marginally accurate at $\tau \sim 1$, but becomes progressively more precise with decreasing τ . However, since the photon intensity is sharply forward-peaked in the lab frame, this approximation is better than one might have expected even at $\tau \lesssim 1$. A non-interacting photon preserves its frequency in the lab frame as well as the quantity $(1 - \mu^2)r^2$, where μ is the direction cosine relative to the local radial direction. The phase space density $f_\gamma(k, x)$ is conserved along any photon ray path. Consequently, we need only to relate the photon frequency and direction cosine in the comoving frame at different points in the flow to find E_0 , P_0 , and F_0 at small τ . In the extreme relativistic limit, photons are highly beamed in the forward direction as seen in the lab frame. It is therefore convenient to define the quantity

$$\eta = 2\gamma^2(1 - \mu), \quad (28)$$

in terms of which the direction cosine in the rest frame is approximately $\mu_{\text{rf}} \approx (1 - \eta)/(1 + \eta)$. As η spans the range $[0, \infty]$, μ_{rf} spans the range $[-1, +1]$. From $2(1 - \mu)r^2 = \eta r^2/\gamma^2 \approx \text{constant}$, we get

$$\mu_{\text{rf}} = \frac{1 + \mu_{\text{rf}}^{(1)} - (1 - \mu_{\text{rf}}^{(1)})\zeta(r)}{1 + \mu_{\text{rf}}^{(1)} + (1 - \mu_{\text{rf}}^{(1)})\zeta(r)} \quad (29)$$

where

$$\zeta(r) \equiv \left(\frac{r_1 \gamma}{r \gamma_1} \right)^2. \quad (30)$$

The label ‘1’ denotes a reference point in the flow, taken to be $\tau \sim 1$ below, where we shall assume that the distribution function is known and beyond which photons stream freely. Note that if $\zeta(r) = 1$ then $\mu_{\text{rf}} = \mu_{\text{rf}}^{(1)}$, which means that the direction cosine relative to the local radial direction does not change as long as $\gamma \propto r$; however, as $\zeta(r) \rightarrow 0$, the distribution becomes increasingly peaked around $\mu_{\text{rf}} = 1$. We shall see that $\gamma \propto r$ is maintained to quite small values of τ .

In a similar way, the photon frequency k_{rf} in the rest frame of the flow is

$$k_{\text{rf}} = \frac{k(1 + \eta)}{2\gamma} = k_{\text{rf}}^{(1)} \frac{\gamma_1}{\gamma} \left(\frac{1 + \eta}{1 + \eta_1} \right), \quad (31)$$

or, introducing μ_{rf} rather than η ,

$$k_{\text{rf}} = k_{\text{rf}}^{(1)} \frac{\gamma_1}{\gamma} \left[\frac{1 + \mu_{\text{rf}}^{(1)} + (1 - \mu_{\text{rf}}^{(1)})\zeta(r)}{2} \right]. \quad (32)$$

Now assume that the photon distribution function is $f_\gamma(k_{\text{rf}}^{(1)}, \mu_{\text{rf}}^{(1)})$ at r_1 . If the photons flow freely outside r_1 , then at any larger value of r , the Liouville theorem implies that the phase space distribution is still $f_\gamma(k_{\text{rf}}^{(1)}, \mu_{\text{rf}}^{(1)})$. Only the mapping from r_1 to r is needed to find E_0, P_0 and F_0 .

Suppose the distribution function for the radiation at r_1 can be expanded in terms of orthonormal Legendre polynomials:

$$f_\gamma(k_{\text{rf}}^{(1)}, \mu_{\text{rf}}^{(1)}) = f_0(k_{\text{rf}}^{(1)}) + \mu_{\text{rf}}^{(1)} f_1(k_{\text{rf}}^{(1)}) + \left(\frac{3(\mu_{\text{rf}}^{(1)})^2 - 1}{2} \right) f_2(k_{\text{rf}}^{(1)}) \quad (33)$$

Defining

$$I_1 \equiv \int dq q^3 f_0(q) \quad 2J_1 \equiv \int dq q^3 f_1(q) \quad \text{and} \quad 10K_1 \equiv \int dq q^3 f_2(q), \quad (34)$$

the radiation energy, flux, and pressure can be expressed as:

$$E_0 = \frac{4\pi}{3} \left(\frac{r_1 \gamma_1}{r \gamma} \right)^2 \left\{ I_1 [1 + \zeta(r) + \zeta^2(r)] + J_1 [1 - \zeta^2(r)] + K_1 [1 - \zeta]^2 \right\} \quad (35)$$

$$F_0 = \frac{4\pi}{3} \left(\frac{r_1 \gamma_1}{r \gamma} \right)^2 \left\{ I_1 [1 - \zeta^2(r)] + J_1 [1 + \zeta^2(r)] + K_1 [1 - \zeta^2] \right\} \quad (36)$$

$$P_0 = \frac{4\pi}{3} \left(\frac{r_1 \gamma_1}{r \gamma} \right)^2 \left\{ I_1 [1 - \zeta(r) + \zeta^2(r)] + J_1 [1 - \zeta^2(r)] + K_1 [1 + \zeta]^2 \right\}. \quad (37)$$

We can check that in the stationary frame $r^2 F(r) = \text{constant}$, consistent with energy conservation.

For our purposes, the reference radius r_1 will be taken to be the position of the photosphere. The radiation field is then given by an isotropic blackbody distribution for $r \leq r_1$. (In Section 5, we estimate deviations from a blackbody.) We therefore specialize to $f_1 = f_2 = 0$ (i.e. $J_1 = K_1 = 0$) in the following discussion.

As long as $\zeta(r) = 1$, $E_0 = 3P_0$ and $F_0 = 0$. However, as $\zeta(r) \rightarrow 0$, $P_0 \rightarrow E_0$ and $F_0 \rightarrow E_0$; only when $\gamma \rightarrow \text{constant}$ do P_0, E_0 and F_0 decrease like r^{-2} . Note that one can rewrite the prefactor in equations (35–37) as

$$\left(\frac{r_1 \gamma_1}{r \gamma} \right)^2 = \frac{(r_1/r)^4}{\zeta(r)}; \quad (38)$$

consequently, when $\zeta(r) = 1$, the rest frame energy density and pressure both decrease like r^{-4} . This is so even though there is no interaction with matter. The situation is the same as in expanding universe cosmology, where the radiation field maintains its equilibrium form after it decouples from the matter entirely. We see from the above that when the optical depth is small, the critical function that determines the approach to $F_0/E_0 = 1$ and $P_0/E_0 = 1$ is $\zeta(r)$.

For the pairs, we always solve the annihilation equation derived in the previous subsection.

3. Analytical Model

In this section we will do back-of-the-envelope calculations and obtain approximate results and scaling laws in four different regimes, each characterized by their local temperature T and optical depth τ : First, in the high temperature limit ($T \gg m_e$), electrons, positrons and photons are in equilibrium, the optical depth is very large and we get simple power laws for $\gamma(r)$ and $T(r)$. As the temperature drops below m_e , the number density of electrons and positrons starts to deviate from its equilibrium value and will be calculated approximatively from the annihilation equation. In the region where the optical depth $\tau < 1$, we estimate how the radiation fields affect the velocity and the temperature of the matter. Finally, we calculate the asymptotic values for γ , Tr and $n_e r^2$ for $\tau \rightarrow 0$. A summary of the scaling laws can be found in Fig. 1. The validity of the simple analytical model presented here will be checked against a numerical solution of the equations in the following section. There we will explore models with a range of different initial temperatures and Lorentz factors.

3.1. $\tau \gg 1$ and $T \gg m_e$

When $T \gg m_e$, the radiation energy E_0 is given by the equilibrium Planck energy density, $E_0 = (\pi^2/15)T^4 \equiv aT^4 = 3P_0$. The radiation flux is negligible since the optical depth $\tau \gg 1$; we will check the consistency of this assumption later. (See Section 3.3 for calculations of the optical depth.)

Introduce the notation

$$\rho \equiv \rho_M + E_0 \equiv \rho_{e^-} + \rho_{e^+} + E_0 \quad \text{and} \quad P \equiv P_M + P_0 \equiv P_{e^-} + P_{e^+} + P_0. \quad (39)$$

Energy conservation, equation (10), now simplifies to

$$\frac{d}{dr} \left\{ r^2 (\rho + P) \gamma \sqrt{\gamma^2 - 1} \right\} = 0, \quad \text{i.e.} \quad L \equiv 4\pi r^2 \gamma \sqrt{\gamma^2 - 1} (\rho + P) = \text{constant}. \quad (40)$$

The Euler equation, equation (11), becomes

$$(\rho + P) \frac{d \ln \gamma}{dr} + \frac{dP}{dr} = 0, \quad (41)$$

where we made use of energy conservation (equation [40]).

When ρ and P depend on T alone, $dP/dT = (\rho + P)/T$ (e.g. Weinberg 1972, Section 15.6), and the flow equations give

$$\frac{d \ln(\gamma T)}{d \ln r} = 0; \quad \gamma T = \text{constant} = \gamma_i T_i, \quad (42)$$

and

$$\frac{d \ln \gamma}{d \ln r} = \frac{2}{(Td\rho/dT)/(\rho + P) - \gamma^2/(\gamma^2 - 1)} = \frac{2(\gamma^2 - 1)}{2\gamma^2 - 3}. \quad (43)$$

The last step in the above equation is valid for $\rho = 3P \propto T^4$. For $\gamma \gg 1$, $d \ln \gamma / d \ln r = 1$, i.e.

$$\gamma \propto r; \quad T \propto \frac{1}{r}; \quad \gamma T = \gamma_i T_i \quad \text{for } T \gg m_e \quad (44)$$

(e.g. Goodman 1986; Paczyński 1986). Note that equation (43) requires a minimum initial velocity for the flow to lift off: Demanding $d \ln \gamma / d \ln r > 0$ implies that $\gamma_i > \sqrt{3/2}$.

3.2. $\tau \gg 1$ and $T \sim m_e$

When $T \gg m_e$, $\rho_M (= 3P_M)$ is comparable to $E_0 (= 3P_0)$ and also proportional to T^4 , but for $T \ll m_e$, $\rho_M \ll E_0$. In this subsection we want to explore what happens when $T \lesssim m_e$. Define

$$h(T) \equiv \rho_M + P_M + E_0 + P_0 \approx \begin{cases} \frac{11}{3} \frac{\pi^2}{15} T^4 & \text{for } T \gg m_e \\ \frac{4}{3} \frac{\pi^2}{15} T^4 & \text{for } T \ll m_e. \end{cases} \quad (45)$$

In general, ρ_M and P_M should be found from equations (4) and (5).

We can now calculate the radius r_m where the temperature equals the electron mass, using conservation of energy:

$$\frac{r_m}{r_i} = \sqrt{\frac{\gamma_i \sqrt{\gamma_i^2 - 1} h(T_i)}{\gamma_m \sqrt{\gamma_m^2 - 1} h(m_e)}} = \left(1 - \frac{1}{\gamma_i^2}\right)^{1/4} \frac{m_e}{T_i} \sqrt{\frac{h(T_i)}{h(m_e)}} \approx \left(1 - \frac{1}{\gamma_i^2}\right)^{1/4} \frac{T_i}{m_e} \quad (46)$$

Here $\gamma_m \gg 1$ and $\gamma_m m_e \approx \gamma_i T_i$ was used. Note that the pair density is still close to equilibrium when $T \sim m_e$, which will be verified later in this subsection.

As T drops below m_e , the equilibrium density of electrons and positrons falls off exponentially as

$$n_{e,\text{eq}} \approx \frac{2}{(2\pi)^{3/2}} (m_e T)^{3/2} \exp(-m_e/T). \quad (47)$$

Consequently, for $T \ll m_e$, $\rho_e, P_e \ll E_0, P_0$, and $\rho \approx E_0 \approx 3P \approx 3P_0 \approx (\pi^2/15)T^4$. But then we get the same scaling laws as in the high temperature limit (see the justification of equations [42]-[44]):

$$\gamma \propto r; \quad T \propto \frac{1}{r}; \quad \gamma T = \text{constant} \quad \text{for } T \ll m_e. \quad (48)$$

As long as equilibrium is maintained, the equation of state of the flow is purely a function of temperature, and the Euler equation implies that $\gamma T = \text{constant}$. At the same time, energy conservation requires

$$L \approx 4\pi r^2 h(T) \gamma \sqrt{\gamma^2 - 1} \approx 4\pi r^2 (\gamma_i T_i)^2 T^2 \alpha = \text{constant}. \quad (49)$$

Thus, $r^2 T^2 \alpha = \text{constant}$, resulting in the scaling laws

$$\gamma \approx \gamma_i (r/r_i) \quad \text{and} \quad T \approx T_i (r_i/r) \quad \text{for } T \gg m_e; \quad (50)$$

$$\gamma \approx \gamma_i (r/r_i) \sqrt{4/11} \quad \text{and} \quad T \approx T_i (r_i/r) \sqrt{11/4} \quad \text{for } T \ll m_e. \quad (51)$$

The change in slope is due to the fact that pairs contribute little to $\rho + P$ once they become non-relativistic. This remains true for small $T < m_e$ even though e^\pm are far more plentiful than in pair equilibrium.

At somewhat larger radius than r_m , deviations from pair annihilation equilibrium will become important. (Lee & Weinberg (1977) considered the analogous problem for heavy leptons in the early universe.) In order to estimate where this happens, let us assume that the deviations are small, i.e. $\delta n_e \equiv n_e - n_{e,\text{eq}} \ll n_{e,\text{eq}}$. Then expand $n_e^2 - n_{e,\text{eq}}^2 \approx 2n_{e,\text{eq}}\delta n_e$ in the pair equation (16) to get

$$\delta n_e \approx -\frac{1}{2r^2\langle\sigma_{\text{ann}}v\rangle n_{e,\text{eq}}} \frac{d}{dr} \left\{ n_{e,\text{eq}} r^2 \sqrt{\gamma^2 - 1} \right\}. \quad (52)$$

Since $\gamma \propto r$ as long as equilibrium is maintained, we get

$$\delta n_e \approx -\frac{\gamma}{2r\langle\sigma_{\text{ann}}v\rangle} \left[3 + \frac{d \ln n_{e,\text{eq}}}{d \ln r} \right]. \quad (53)$$

From the exponential form of $n_{e,\text{eq}}$, $d \ln n_{e,\text{eq}}/d \ln r = -d \ln n_{e,\text{eq}}/d \ln T \approx -m_e/T$ for $T \ll m_e$.

Equilibrium fails when δn_e becomes comparable to $n_{e,\text{eq}}$. Let r_{eq} (and T_{eq}) be the radius (and temperature) where $\delta n_e = n_{e,\text{eq}}$; then

$$\frac{2}{(2\pi)^{3/2}} (m_e T_{\text{eq}})^{3/2} \exp(-m_e/T_{\text{eq}}) = \frac{\gamma_{\text{eq}}}{2r_{\text{eq}}\pi r_e^2} \frac{m_e}{T_{\text{eq}}} \quad (54)$$

to leading order in m_e/T_{eq} . Relate T_{eq} and r_{eq} by $T_{\text{eq}} r_{\text{eq}} \sim \sqrt{11/4} m_e r_m$, and use $\gamma_{\text{eq}}/r_{\text{eq}} \approx \sqrt{4/11} \gamma_i/r_i$ (from the limiting cases of $h(T)$, assuming $T_{\text{eq}} \ll m_e$ and $T_i > m_e$, and $\gamma\sqrt{\gamma^2 - 1} \approx \gamma^2$ in the energy conservation equation). We then find

$$\frac{2}{(2\pi)^{3/2}} m_e^3 \left(\frac{11}{4}\right)^{3/4} \left(\frac{r_m}{r_{\text{eq}}}\right)^{3/2} \exp(-\sqrt{4/11} r_{\text{eq}}/r_m) = \frac{(4/11)(\gamma_i/r_i) r_{\text{eq}}}{2\pi r_e^2} \frac{r_{\text{eq}}}{r_m}, \quad (55)$$

which has the approximate solution

$$r_{\text{eq}}/r_m \approx \sqrt{11/4} \ln \left[\sqrt{2/\pi} (11/4)^{7/4} (r_e^2 r_i m_e^3) / \gamma_i \right] - \sqrt{11/4} (5/2) \ln \left[\frac{r_{\text{eq}}}{r_m} \right]. \quad (56)$$

Note that r_{eq}/r_m does not depend on the initial temperature T_i and is only weakly dependent on γ_i . For $r_i = 10^6 \text{cm}$, the numerical value is $r_{\text{eq}}/r_m \approx 33 - \sqrt{11/4} \ln \gamma_i$. The temperature at r_{eq} is approximately $T_{\text{eq}} \sim \sqrt{11/4} m_e r_m / r_{\text{eq}} \sim 0.052 m_e$.

3.3. $\tau \sim 1$ and $T \ll m_e$

At r_{eq} the energy density of the flow is dominated by the photons: Since $T_{\text{eq}} \ll m_e$ we have

$$\frac{\rho_{\text{M,eq}}}{E_{0,\text{eq}}} \approx \frac{2m_e n_e(r_{\text{eq}})}{(\pi^2/15) T_{\text{eq}}^4} \approx 1.1 \times 10^{-6} \gamma_i. \quad (57)$$

As long as the flow remains photon dominated and the radiation field stays close to its blackbody form, $\gamma \propto r$.

Now, let us estimate the optical depth in the flow. In the rest frame of the flow, the density of electrons and positrons is $2n_e \equiv n_- + n_+$ and the cross section for interaction is $(\sigma_s + \sigma_a)$. A reasonable choice for the optical depth of the flow is the radial depth (Abramowicz, Novikov & Paczyński 1991)

$$\frac{d\tau}{dr} = 2n_e(\sigma_s + \sigma_a) \sqrt{\frac{1-v}{1+v}} \approx \frac{n_e(\sigma_s + \sigma_a)}{\gamma}, \quad (58)$$

where the last approximation holds for an extremely relativistic flow. We then find

$$\tau(r) = \frac{8\pi}{3} r_e^2 \left(\frac{\sigma_a}{\sigma_T} + \frac{\sigma_s}{\sigma_T} \right) \int_r^\infty dr \frac{n_e(r)}{\gamma(r)}. \quad (59)$$

As long as the radiation field remains close to a blackbody, $\gamma(r) \approx \gamma_{\text{eq}}(r/r_{\text{eq}})$. Since $n_e > n_{e,\text{eq}}$ outside r_{eq} , we can approximate the pair equation as

$$\frac{1}{r^2} \frac{d}{dr} (n_e r^3) \approx -\pi r_e^2 \frac{r_{\text{eq}}}{\gamma_{\text{eq}}} n_e^2. \quad (60)$$

In other words, although pair annihilation continues outside r_{eq} , pair creation becomes unimportant as the number of photons energetic enough to produce e^\pm pairs decreases exponentially. The solution to this equation is

$$n_e(r) \approx \frac{n_e(r_{\text{eq}})}{1 + (1/3)\sqrt{4/11}(r_{\text{eq}}/r_m) \left[1 - (r_{\text{eq}}/r)^3 \right]} \left(\frac{r_{\text{eq}}}{r} \right)^3 \quad (61)$$

for $r > r_{\text{eq}}$ and $\gamma \propto r$. Since $n_e(r_{\text{eq}}) \sim n_{e,\text{eq}}(r_{\text{eq}}) + \delta n_e(r_{\text{eq}}) \sim 2\delta n_e(r_{\text{eq}}) \sim (4/11)(\gamma_i/r_i)(r_{\text{eq}}/r_m)/\pi r_e^2$,

$$\begin{aligned} \tau(r) &\approx \frac{8\pi}{3} r_e^2 \left(\frac{\sigma_a}{\sigma_T} + \frac{\sigma_s}{\sigma_T} \right) \frac{r_{\text{eq}}}{\gamma_{\text{eq}}} n_e(r_{\text{eq}}) r_{\text{eq}}^3 \int_r^\infty \frac{dr}{r^4 \left\{ 1 + (1/3)\sqrt{4/11}(r_{\text{eq}}/r_m) \left[1 - (r_{\text{eq}}/r)^3 \right] \right\}} \\ &= -\frac{8}{3} \left(\frac{\sigma_a}{\sigma_T} + \frac{\sigma_s}{\sigma_T} \right) \ln \left\{ 1 - \frac{(1/3)\sqrt{4/11}(r_{\text{eq}}/r_m) (r_{\text{eq}}/r)^3}{1 + (1/3)\sqrt{4/11}(r_{\text{eq}}/r_m)} \right\} \end{aligned} \quad (62)$$

at $r > r_{\text{eq}}$. The photospheric radius r_{ph} may be estimated from $\tau(r = r_{\text{ph}}) = 1$, implying

$$\frac{r_{\text{ph}}}{r_{\text{eq}}} = \left\{ \left(3\sqrt{\frac{11}{4}} \frac{r_m}{r_{\text{eq}}} + 1 \right) \left[1 - \exp \left(-\frac{3\sigma_T}{8[\sigma_a + \sigma_s]} \right) \right] \right\}^{-1/3} \quad (63)$$

For example, if $\sigma_a + \sigma_s \sim \sigma_T$ then $r_{\text{ph}}/r_{\text{eq}} \sim 1.4$. This implies that the temperature at the photosphere is $T_{\text{ph}}/m_e \approx (r_{\text{eq}}/r_{\text{ph}})T_{\text{eq}}/m_e \sim 0.037$. The optical depth at r_{eq} is $\tau_{\text{eq}} \sim 5.4(\sigma_a + \sigma_s)/\sigma_T$.

Outside r_{ph} the photons stream nearly freely out to the observer. The escaping photons form a high energy gamma ray continuum since $T\gamma$, the temperature seen by a distant observer in the lab frame, is approximately constant in the flow out to r_{ph} .

3.4. $\tau < 1$ and $T \ll m_e$

For $\tau < 1$, energy and momentum may still be deposited by photons in the pair wind. Thus, the pairs can be accelerated and heated via their interactions with escaping photons even though the wind is not opaque. Because the energy and momentum in pairs is smaller than in radiation at $\tau \sim 1$, even small depositions of energy and momentum may affect the pairs significantly. In this regime, each electron or positron experiences a force

$$f_{\text{rf}}^r \approx (\sigma_a + \sigma_s)F_0 \quad (64)$$

in the flow rest frame. (Since $T \ll m_e$, there is little difference between rest frames of flow and individual electrons.) Transforming to the observer's frame implies

$$\frac{d\gamma}{dr} \approx (\sigma_a + \sigma_s)F_0/m_e, \quad (65)$$

where we used $d\tau = dt/\gamma$ and $dt = vdr \approx dr$. This can also be seen from the dynamical equation (26). The appropriate flux in this regime is given by the free-streaming limit,

$$F_0 = \frac{4\pi}{3} \left(\frac{r_1\gamma_1}{r\gamma} \right)^2 I_1[1 - \zeta^2(r)], \quad (66)$$

assuming, for simplicity, that the radiation field at r_1 is isotropic, as will be the case when matching onto blackbody radiation at $\tau \sim 1$. Define $z \equiv r/r_i$ and

$$\Lambda \equiv \frac{4\pi}{3} \left(\frac{\sigma_a}{\sigma_T} + \frac{\sigma_s}{\sigma_T} \right) (\sigma_T r_i m_e^3) \frac{I_1}{m_e^4 \gamma_1} \frac{z_1}{\gamma_1} \approx 3.1 \times 10^7 \left(\frac{\sigma_a}{\sigma_T} + \frac{\sigma_s}{\sigma_T} \right) \frac{1}{\gamma_i} \frac{r_i}{10^6 \text{cm}} \left(\frac{r_{\text{eq}}}{r_{\text{ph}}} \right)^4. \quad (67)$$

Since $\gamma/\gamma_1 = (z/z_1)\sqrt{\zeta}$, the equation of motion becomes

$$1 + \frac{1}{2\zeta} \frac{d\zeta}{d \ln z} = \Lambda \left(\frac{z_1}{z} \right)^4 \zeta^{-3/2} (1 + \zeta)(1 - \zeta). \quad (68)$$

At the photosphere, $z = z_1$ and $\zeta = 1$. Since $\Lambda \gg 1$, ζ will remain close to one until $2\Lambda(z_1/z)^4 \sim 1$. Thus, $\gamma \propto r$ until $z = z_\gamma$, where

$$\frac{z_\gamma}{z_1} \sim \Lambda^{1/4}, \quad (69)$$

note that for $z_1 = r_{\text{ph}}/r_i$, $r_\gamma/r_i \sim 2 \times 10^3 T_i/m_e$ for γ_i and $(\sigma_a + \sigma_s)/\sigma_T$ of order unity. In this simplified model, $\gamma \rightarrow \gamma_\infty$, the asymptotic Lorentz factor, for $z > z_\gamma$. Moreover $\gamma_\infty/z_\gamma \sim \gamma_1/z_1$, so

$$\gamma_\infty \approx \gamma_1 \Lambda^{1/4}. \quad (70)$$

The resulting ‘boost’ γ_∞/γ_1 may be large: For example if $\gamma_i \sim 2$ and $\sigma_a + \sigma_s \sim \sigma_T$, then $\Lambda \sim 4 \times 10^6$, and the asymptotic Lorentz factor of the flow increases by a factor of ~ 45 as compared to its value at the photosphere! Specifically, by using previous estimates for the flow variables at $\tau > 1$, we get

$$\gamma_\infty \sim 1.4 \times 10^3 \gamma_i^{3/4} \frac{T_i}{m_e} \left(\frac{\sigma_a}{\sigma_T} + \frac{\sigma_s}{\sigma_T} \right)^{1/4} \left(\frac{r_i}{10^6 \text{cm}} \right)^{1/4}. \quad (71)$$

We are now in a position to justify our assertion that the radiation field will stay close to blackbody in the comoving frame long after the optical depth drops below unity. In the free streaming limit the radiation energy, flux and pressure remain close to their equilibrium values as long as $\zeta - 1$ is small, which will be the case until $r \sim r_\gamma$. For $r > r_\gamma$, $\gamma \rightarrow \gamma_\infty$, and the right-hand side in the pair equation can be neglected. This is because annihilation becomes unimportant for $r > r_\gamma$ because of the low number density of pairs, as can be easily checked. Thus, for $r > r_\gamma$, $n_e r^2 \sim \text{constant}$ and the optical depth at r_γ becomes $\tau(r_\gamma) \equiv \tau_\gamma \approx n_e(r_\gamma)(r_\gamma/\gamma_\infty)(\sigma_a + \sigma_s)$. Using our previous results, we find that little deviation from blackbody radiation develops until $\tau_\gamma \sim 1.7 \times 10^{-5} \left(\frac{\sigma_a}{\sigma_T} + \frac{\sigma_s}{\sigma_T} \right)^{1/4} \gamma_i^{3/4}$.

Finally, we need to estimate the asymptotic number density of pairs. Equation (61) gives the approximate number density for $r_{\text{eq}} < r < r_\gamma$, where $\gamma \propto r$:

$$n_e(r) \approx \frac{(4/11)(\gamma_i/r_i)(r_{\text{eq}}/r_m)(1/\pi r_e^2)}{1 + (1/3)\sqrt{4/11}(r_{\text{eq}}/r_m)[1 - (r_{\text{eq}}/r)^3]} \left(\frac{r_{\text{eq}}}{r} \right)^3 \quad \text{for } r > r_{\text{eq}}; \gamma \propto r. \quad (72)$$

For $z > z_\gamma$ the pair equation reduces to

$$n_e(r)z^2 \approx n_e(r_\gamma)z_\gamma^2 \approx n_e(r_\gamma)z_{\text{ph}}^2 \Lambda^{1/2}. \quad (73)$$

Using the approximate results for $n_e(r_\gamma)$, r_m/r_i , r_{eq}/r_m and $r_{\text{ph}}/r_{\text{eq}}$, we find

$$n_e \sim 8.6 \times 10^{19} \left(\frac{T_i}{m_e} \right)^2 (\gamma_i)^{5/4} \left(\frac{\sigma_a}{\sigma_T} + \frac{\sigma_s}{\sigma_T} \right)^{-1/4} \left(\frac{r}{r_i} \right)^{-2} \text{ cm}^{-3} \quad (74)$$

for $r > r_\gamma$.

The acceleration of the pair wind increases the energy outflow in pairs to a fraction $L_e/L \approx 45r^2\gamma^2\rho_M/11\pi^2r_i^2\gamma_i^2T_i^4$ of the total luminosity. Using $\rho_M \approx 2m_en_e$ and earlier estimates for the other quantities in the above ratio, we find

$$L_e/L \sim 8.5 \times 10^{-6} (\gamma_i)^{3/4} \left(\frac{\sigma_a}{\sigma_T} + \frac{\sigma_s}{\sigma_T} \right)^{1/4} \quad (75)$$

for $r > r_\gamma$. We conclude that for reasonable γ_i the flow never becomes matter dominated. Almost all of the original L is carried away by photons. Notice that although the asymptotic pair density and Lorentz factor depend on both γ_i and T_i , the value of L_e/L at $r \gg r_\gamma$ depends only on γ_i .

To find the asymptotic behavior of the temperature of pairs, consider the entropy per particle, $Tds = P_M d(1/2n_e) + d(\rho_M/2n_e)$. For $T \ll m_e$, $P_M \approx 2n_eT$ and $\rho_M \approx 2m_en_e + 3n_eT$. Since $n_e \propto r^{-2}$ for large r we have

$$Tds \approx \frac{2}{r}Tdr + \frac{3}{2}dT. \quad (76)$$

Adiabatic cooling, $s=\text{constant}$, would result in $T \propto r^{-4/3}$ (as could also be obtained from $T \propto n^{2/3}$ and $n \propto r^{-2}$). However, energy is still deposited by photons in the e^\pm flow even at $r > r_\gamma$; the amount of radiative energy input per particle in a time $t_r \sim r/\gamma$ is

$$dq = -G_0^0 t_r / 2n_e \approx -G_0^0 r / 2n_e \gamma. \quad (77)$$

For $r > r_\gamma$, $E_0 \approx F_0 \approx P_0$ and energy conservation implies that $L \approx 4\pi r^2 \gamma^2 [E_0 + P_0 + 2F_0] \approx 16\pi r^2 \gamma^2 E_0$. Consequently, $-G_0^0 \approx 2n_e \sigma_a E_0 \approx 2n_e \sigma_a L / 16\pi r^2 \gamma^2$. Since $T ds = dq$, equation (76) takes the form

$$\frac{d \ln T}{d \ln r} \approx -\frac{4}{3} + \frac{\sigma_a L}{24\pi \gamma^3 r T} \quad (78)$$

with solution

$$T \approx \frac{T_\gamma r_\gamma^{4/3}}{r^{4/3}} + \frac{\sigma_a L (r^{1/3} - r_\gamma^{1/3})}{8\pi \gamma_\infty^3 r^{4/3}}. \quad (79)$$

There are two cases to consider, depending on the relative sizes of the two terms on the right hand side in equation (78); their ratio is $\sigma_a L / 32\pi \gamma_\infty^3 r T \sim 7.5 \times 10^2 (\sigma_a / \sigma_T) \gamma_i^{-1/4} [(\sigma_a + \sigma_s) / \sigma_T]^{-3/4} (r_i / 10^6 \text{cm})$. If this ratio is larger than unity, $T \propto r^{-1}$. If the ratio is much smaller than unity, $T \propto r^{-4/3}$ until a radius $r/r_\gamma \sim (8\pi \gamma_\infty^3 T_\gamma r_\gamma / \sigma_a L)^3 \sim 3.3 \times 10^{-11} (\sigma_a / \sigma_T)^{-3} \gamma_i^{3/4} [(\sigma_a + \sigma_s) / \sigma_T]^{9/4} (r_i / 10^6 \text{cm})^{-3}$, after which $T \propto r^{-1}$. This result could also have been obtained from equation (27).

3.5. Positronium formation?

To this point, we have considered e^\pm annihilation in flight only. At large radii, e^\pm pairs cool considerably, and it is possible that recombination to positronium occurs, leading ultimately to destruction of the pairs. Like hydrogen recombination, positronium formation would proceed via a free-bound transition to an excited state, followed by a radiative cascade to lower energy states, with increasing probability of pair annihilation. However, in order for this process to be important, the rate at which positronium is formed must exceed the expansion rate of the flow. To estimate the rate of positronium formation, we use the results from hydrogen recombination with the reduced mass $\approx m_e$ replaced by $m_e/2$.

It is straightforward to show that the ‘gross’ recombination rate – ignoring radiative ionization, which leads to a lower ‘net’ recombination rate – is small compared to the expansion rate $\Gamma_{\text{exp}} \sim \gamma/r$ at all points outside r_{eq} . Recall that at r_{eq} , the electron temperature is $T_{\text{eq}} \approx 0.052 m_e \gg e^4 m_e / 4 \equiv \chi_{\text{pos}}$, the ionization potential of positronium. As long as $T \gg \chi_{\text{pos}}$, the recombination coefficient for the n th excited state of positronium is $\Gamma_n = n_e \langle \sigma v \rangle_n$, where (e.g. Rybicki & Lightman 1979)

$$\langle \sigma v \rangle_n \approx \frac{32\sqrt{\pi}}{3\sqrt{3}} \frac{\alpha^3 r_e^2}{n^3} \left(\frac{m_e}{T} \right)^{3/2} \ln \left(\frac{2Tn^2}{\chi_{\text{pos}}} \right). \quad (80)$$

At r_{eq} , we find $\Gamma_1/\Gamma_{\text{exp}} \sim 10^{-3}$; for $n > 1$, the ratio $\Gamma_n/\Gamma_{\text{exp}}$ is even smaller. Moreover, $\Gamma_n/\Gamma_{\text{exp}} \propto n_e T^{-3/2} r/\gamma \propto r^{-3/2}$ outside r_{eq} , but still at radii where $\gamma \propto r$, $T \propto 1/r$ and $T > \chi_{\text{pos}}$. Thus, e^\pm recombination is very slow in this regime.

Ultimately, T drops below χ_{pos} and the recombination rate (summed over all states) is approximately

$$\Gamma_{\text{pos}} \approx 2.08 \times 10^{-13} n_e \lambda^{1/2} (0.429 + (1/2) \ln \lambda + 0.469 \lambda^{-1/3}) \quad (81)$$

where $\lambda = 1.33 \times 10^{-5} m_e/T$ and n_e is in cm^{-3} (e.g. Rybicki & Lightman 1979). In this regime, $\Gamma_{\text{pos}}/\Gamma_{\text{exp}} \propto n_e r/\gamma T^{1/2} \propto 1/r\gamma^2 T^{1/2}$, since $n_e r^2 \gamma \approx \text{constant}$; thus, $\Gamma_{\text{pos}}/\Gamma_{\text{exp}}$ continues to decrease with radius far out in the flow, at first $\propto r^{-5/2}$, and ultimately $\propto r^{-1/2}$. Thus we conclude that the formation of positronium is always very slow, and does not affect the pair density substantially.

4. Results

A large number of models were calculated, covering a wide range of initial temperatures ($1 \leq T_i/m_e \leq 1000$), initial Lorentz factors ($1.25 \leq \gamma_i \leq 10$), and absorption cross-sections ($10^{-6} \leq \sigma_a/\sigma_T \leq 1$). The scattering cross-section was held fixed at $\sigma_s/\sigma_T = 1$, and the initial radius $r_i = 10^6 \text{cm}$. Due to the stiffness in the pair equation, and in the dynamical equations for $\tau < 1$, we used a semi-implicit scheme for solving the system of equations.

Figs 2 and 3 show the ratios r_m/r_i , r_{eq}/r_m , $r_{\text{ph}}/r_{\text{eq}}$ and r_γ/r_{ph} as functions of the initial temperature T_i and Lorentz factor γ_i . The agreement between the numerical results (solid lines) and the approximations from the analytical model (dotted lines) is very good.

Fig. 4 confirms the high asymptotic Lorentz factors as well as their dependence on initial temperature and Lorentz factor, $\gamma_\infty \propto (T_i/m_e)\gamma_i^{3/4}$.

Equation (79) implies that $T \propto 1/r$ for large r ; this is seen in Fig. 5. The behavior of $d \ln T/d \ln r$ can be understood from the dynamical equations $T_{;\beta}^{\alpha\beta} = -G^\alpha$. For $T \ll m_e$, $\rho_M \gg P_M$ and the energy equation can be approximated as

$$\frac{3}{2} \frac{d \ln T}{d \ln r} + 2 + \frac{d \ln \gamma}{d \ln r} \approx \frac{z}{\gamma} (\sigma_T r_i m_e^3) \frac{m_e \sigma_a}{T \sigma_T} \left[\frac{E_0}{m_e^4} - \frac{U_{\text{eq}}}{m_e^4} \right]. \quad (82)$$

The left hand side of this equation contains terms of order unity. If σ_a/σ_T is small enough to make the right hand side much less than 1, we must have $d \ln T/d \ln r \approx -4/3 - (2/3)d \ln \gamma/d \ln r$. For $r < r_\gamma$, where $\gamma \propto r$, $d \ln T/d \ln r$ will therefore tend to approach -2 , as can be seen from Fig. 5 when $\sigma_a/\sigma_T = 10^{-6}$. When $r > r_\gamma$, $\gamma \rightarrow \text{constant}$ and $d \ln T/d \ln r$ approaches $-4/3$. This is also seen in the graph, before heating from the radiation eventually forces T to be proportional to $1/r$. On the other hand, if σ_a/σ_T is large enough to make $(z/\gamma)(\sigma_T r_i m_e^3)(m_e/T)(\sigma_a/\sigma_T) \gg 1$, $E_0/m_e^4 - U_{\text{eq}}/m_e^4$ must be very close to 0. From the free-streaming form of E_0 this means that $T^4 \propto r^{-2}\gamma^{-2}$. Consequently, for $r < r_\gamma$ we have $d \ln T/d \ln r \approx -1$, while for $r > r_\gamma$, $\gamma \sim \gamma_\infty$ and $T \propto r^{-1/2}$. This is seen from the plot of $d \ln T/d \ln r$ for $\sigma_a = \sigma_T$.

Next, Fig. 6 serves as a check of our estimates for the asymptotic number density of pairs, and for the ratio of energy in pairs to the total energy. Again, the analytical model (dotted lines) agrees very well with the numerical results (solid lines).

When $\tau < \tau_\gamma$, i.e. $r > r_\gamma$, the Lorentz factor approaches a constant value, as seen in Fig. 7. The dip in $d \ln \gamma / d \ln r$ for large optical depths happens when $T \sim m_e$, after which pairs contribute little to the total energy. This point is the transition between $\gamma \approx \gamma_i(r/r_i)$, when $T \gg m_e$, and the low-temperature limit $\gamma \approx \gamma_i(r/r_i) \sqrt{4/11}$ (see equations [50] and [51]).

5. Robustness of Blackbody

Here, we show that the deviations from blackbody in the photon distribution function are small. In the $\gamma \gg 1$ limit, the corresponding spectrum observed in the lab frame has a slightly broader peak and a shallower slope for low frequencies compared to a blackbody. We also consider non-radial perturbations to the flow and resulting effects on the observed radiation spectrum.

5.1. Deviations from blackbody in the comoving frame

In this subsection we will give a more careful justification for the simple model we used for the radiation field. When the optical depth is large, the radiation is trapped effectively. Because thermal emission and scattering are isotropic in the rest frame of the flow, one expects the radiation field to be close to isotropic when the optical depth is larger than one. The deviation from isotropy can be treated as a small perturbation on the radiation field in this limit. From Section 2.2, the equation of radiative transfer is

$$k^\beta \frac{\partial}{\partial x^\beta} f_\gamma(k, x) = C_\gamma. \quad (83)$$

The Lorentz invariant collision terms are

$$\mathcal{C}_s = 2n_e \sigma_s \tilde{k}^0 \left[-f_\gamma(k, x) + \int d^2 \hat{n}' g(\hat{n}' \rightarrow \hat{n}) f_\gamma(k', x) \right] \quad \text{and} \quad (84)$$

$$\mathcal{C}_a = 2n_e \sigma_a \tilde{k}^0 [-f_\gamma(k, x) + f_{\text{BB}}(\tilde{k}^0/T)] \quad (85)$$

for scattering and absorption/emission, respectively. Below, we neglect pair production and annihilation since these processes have a negligible effect on the escaping radiation.

Perturbing away from blackbody radiation, we write

$$f_\gamma(k, x) = f_{\text{BB}}(\tilde{k}^0/T) + \delta f_\gamma(k, x). \quad (86)$$

It is convenient to introduce the four-vector $n^\mu = k_\nu P^{\mu\nu} / \tilde{k}^0$, where the projection tensor is $P^{\mu\nu} = g^{\mu\nu} + U^\mu U^\nu$. This four-vector reduces to the unit vector along the direction of propagation in the rest frame of the flow. In terms of n^μ and $\tilde{k}^0 = -k_\mu U^\mu$, we have $k^\mu = \tilde{k}^0 (n^\mu + U^\mu)$.

Now expand the correction to blackbody, δf_γ , in Legendre polynomials:

$$\delta f_\gamma(k, x) = A + B_\mu n^\mu + C_{\mu\nu} \left(\frac{3n^\mu n^\nu - P^{\mu\nu}}{2} \right). \quad (87)$$

Introduce an explicit form for the scattering kernel,

$$g(\hat{\mathbf{n}}' \rightarrow \hat{\mathbf{n}}) = \frac{1 + aP_2(\hat{\mathbf{n}} \cdot \hat{\mathbf{n}}')}{4\pi}, \quad (88)$$

where $P_2(\hat{n}, \hat{n}') = [3(\hat{n} \cdot \hat{n}')^2 - 1]/2$. We will specialize eventually to Thomson scattering for which $a = 1/2$.

With the expansions in equations (86) and (87), the right-hand side of the transfer equation becomes

$$\begin{aligned} C_\gamma &= 2n_e \tilde{k}^0 \left\{ -\sigma_a A - (\sigma_a + \sigma_s) B_\mu n^\mu \right. \\ &\quad \left. - \left[\sigma_a + \sigma_s \left(1 - \frac{a}{5} \right) \right] C_{\mu\nu} \left(\frac{3n^\mu n^\nu - P^{\mu\nu}}{2} \right) \right\} + C_p. \end{aligned} \quad (89)$$

On the left hand side one gets

$$\begin{aligned} &k^\beta \frac{\partial}{\partial x^\beta} f_{\text{BB}}(\tilde{k}^0/T(x)) = \\ &-\tilde{k}^0 \psi(\tilde{k}^0/T) \left[U^\nu \frac{T_{,\nu}}{T} + \frac{P^{\mu\nu}}{3} U_{\mu;\nu} + n^\mu \left(\frac{T_{,\mu}}{T} + U^\nu U_{\mu;\nu} \right) + \frac{2}{3} \left(\frac{3n^\mu n^\nu - P^{\mu\nu}}{2} \right) U_{\mu;\nu} \right] \end{aligned} \quad (90)$$

with $\psi(z) \equiv z f'_{\text{BB}}(z)$. Equating equations (89) and (90), the results for A, B_μ and $C_{\mu\nu}$ can be read off. This allows us to find the energy momentum tensor for radiation,

$$T_R^{\mu\nu} = \int \frac{d^3k}{k^0} k^\mu k^\nu \left[f_{\text{BB}}(-k^\lambda U_\lambda/T(x)) + A + B_\lambda n^\lambda + C_{\lambda\sigma} \left(\frac{3n^\lambda n^\sigma - P^{\lambda\sigma}}{2} \right) \right]. \quad (91)$$

The results are

$$\begin{aligned} \delta \tilde{E}_0 &\equiv \frac{E_0 - U_{\text{eq}}}{U_{\text{eq}}} = -4t_0 \left\{ \frac{1}{\gamma T} \frac{d}{d \ln r} (T \sqrt{\gamma^2 - 1}) - \frac{2}{3} \frac{r}{\gamma} \frac{d}{d \ln r} \left(\frac{\sqrt{\gamma^2 - 1}}{r} \right) \right\} \\ &+ t_0 \frac{r}{\gamma} G_{\text{p},0}^0 \frac{1}{U_{\text{eq}}} \end{aligned} \quad (92)$$

$$\delta \tilde{F}_0 \equiv \frac{F_0}{U_{\text{eq}}} = -\frac{4}{3} t_1 \frac{1}{\gamma T} \frac{d}{d \ln r} (\gamma T) \quad (93)$$

$$\delta \tilde{P}_0 \equiv \frac{P_0 - U_{\text{eq}}/3}{U_{\text{eq}}} = \frac{\delta \tilde{E}_0}{3} - \frac{16}{45} t_2 \frac{r}{\gamma} \frac{d}{d \ln r} \left(\frac{\sqrt{\gamma^2 - 1}}{r} \right). \quad (94)$$

where

$$t_0 \equiv -\frac{\gamma}{r} \frac{\pi}{2n_e a T^4} \int_0^\infty \frac{d\tilde{k}^0 (\tilde{k}^0)^3 \psi(\tilde{k}^0/T)}{\sigma_a} \quad (95)$$

$$t_1 \equiv -\frac{\gamma}{r} \frac{\pi}{2n_e a T^4} \int_0^\infty \frac{d\tilde{k}^0 (\tilde{k}^0)^3 \psi(\tilde{k}^0/T)}{\sigma_a + \sigma_s} \quad (96)$$

$$t_2 \equiv -\frac{\gamma}{r} \frac{\pi}{2n_e a T^4} \int_0^\infty \frac{d\tilde{k}^0 (\tilde{k}^0)^3 \psi(\tilde{k}^0/T)}{\sigma_a + \sigma_s (1 - a/5)} \quad (97)$$

with $U_{\text{eq}} = \pi^2 T^4/15$ as before.

From the analytical model as well as the numerical results we know that $\gamma T = \text{constant}$ and $\gamma \propto r$ are excellent approximations for $r < r_\gamma$. Then $\delta \tilde{F}_0 = 0$, $\delta \tilde{E}_0 \sim \mathcal{O}(t_0/\gamma^2)$ and $\delta \tilde{P}_0 \sim \mathcal{O}(t_2/\gamma^2)$ when $\gamma \gg 1$; since t_0^{-1} and t_2^{-1} are of the same order as the absorption and total optical depth, respectively, we see that the corrections to blackbody radiation are negligible when $\gamma \gg 1$.

These results are also consistent with a more careful treatment of the equation of radiative transfer. This equation is most conveniently written as

$$\left[\frac{\partial}{\partial r} + \frac{2(1-\lambda)}{r} \left(\frac{r}{\gamma} \frac{d\gamma}{dr} - 1 \right) \left(q \frac{\partial}{\partial q} - \lambda \frac{\partial}{\partial \lambda} \right) \right] f_\gamma(q, \lambda, r) = \frac{n_e(\sigma_a + \sigma_s)}{\gamma \lambda} \left[-f_\gamma(q, \lambda, r) + \epsilon f_{\text{BB}}(q/\gamma T) + (1-\epsilon) \int_0^{+1} d\lambda' f_\gamma(q, \lambda', r) \right] \quad (98)$$

in an extremely relativistic flow (Grimsrud 1998). Here $\epsilon \equiv \sigma_a/(\sigma_a + \sigma_s)$, $\eta \equiv 2\gamma^2(1-\mu)$, $\lambda \equiv 1/(1+\eta)$ and $q \equiv k/2\lambda$, with μ the direction cosine and k the photon energy in the lab frame. Again, the contribution from pairs is neglected on the right hand side of the transfer equation. The left hand side of this equation simplifies considerably when $\gamma \propto r$. If, in addition, $\gamma T = \text{constant}$, we see that $f_\gamma(q, \lambda, r) = f_{\text{BB}}(q/\gamma T)$ is the solution for the distribution function. Thus, as long as these two conditions are satisfied, the deviation from blackbody radiation vanishes in the high- γ limit up to terms of order $\mathcal{O}(1/\gamma^2)$ which we have neglected. Note that equation (98) holds for both large and small optical depths.

It is interesting to contrast the high- γ limit of equations (92)-(94) with a static atmosphere, where $\gamma = 1$. In the static case, neglecting pair-heating,

$$\delta \tilde{E}_0 = 0, \quad \delta \tilde{F}_0 = -\frac{4}{3} t_1 \frac{d \ln T}{d \ln r}, \quad \text{and} \quad \delta \tilde{P}_0 = 0 \quad (99)$$

in the diffusion approximation, $\tau \gg 1$. Often one relates the radiation pressure to the radiation energy via a variable Eddington factor $f_{\text{Edd}}(\tau)$, $P_0 = E_0[1/3 + f_{\text{Edd}}(\tau)]$. This is a closure relation needed for the first two moment equations obtained from the equation of radiative transfer. The above relations constrain the form of $f_{\text{Edd}}(\tau)$. For $\tau \gg 1$, $f_{\text{Edd}}(\tau)$ must be at least quadratic in $1/\tau$; the linear term vanishes in this limit.

Recall from Section 3.4 that a free-streaming radiation field, coupled to the matter via the dynamical equations $T_{M;\beta}^{\alpha\beta} = -G^\alpha$, resulted in $\gamma \propto r$ and consequently a radiation field close to blackbody out to optical depths much less than 1. This behavior is then also consistent with the full radiative transfer equation as discussed above. Furthermore, note that since deviations from blackbody in the radiation fields start building up only when $\tau \ll 1$, we cannot use a variable Eddington factor $f_{\text{Edd}}(\tau)$ in our extremely relativistic atmosphere.

5.2. Observed spectrum

To compute the observed spectrum, we use the fact that the (comoving frame) photon distribution function is blackbody to a very good approximation at any τ for $\gamma \propto r$. This allows us to find the radially directed flux per energy interval seen by a stationary observer at arbitrary r , using

$$\frac{dF}{dp} = \frac{p^3}{2\pi^2} \int_{-1}^1 \frac{\mu d\mu}{\exp[\gamma p(1 - v\mu)/T] - 1} \quad (100)$$

where $\gamma \propto r$ (and p is the observer-frame photon energy) and T is the blackbody temperature in the frame moving radially with Lorentz factor γ . (The same results can be found from free streaming at $\tau < 1$.) For $\gamma \gg 1$, the integral can be done analytically to give

$$\frac{dF}{dp} \approx \frac{p^2 T}{2\pi^2 \gamma} \{-\ln[1 - \exp(-p/2\gamma T)]\}. \quad (101)$$

At small values of $p/\gamma T$, this expression tends to

$$\frac{dF}{dp} \approx \frac{p^2 T}{2\pi^2 \gamma} \ln(2\gamma T/p); \quad (102)$$

at large values of $p/\gamma T$ it tends to

$$\frac{dF}{dp} \approx \frac{p^2 T}{2\pi^2 \gamma} \exp(-p/2\gamma T). \quad (103)$$

In order to compare (101) with a blackbody that fits the observed flux best, we minimize the integral

$$S(B_0, x_0) = \int_0^\infty dx \left\{ -x^2 \ln[1 - \exp(-x)] - \frac{B_0 x^3}{\exp(x/x_0) - 1} \right\}^2 \quad (104)$$

with respect to the two parameters B_0 and x_0 . The two functions are plotted in Fig. 8. Compared to a blackbody, the observed flux is seen to have a broader peak, and a shallower slope at low photon energies. A similar result was found by Goodman (1986) from his fireball simulations.

5.3. Perturbations about spherical symmetry

So far we have assumed the flow to be static and spherically symmetric. In reality, however, these assumptions break down if the flow is affected by, e.g., a magnetic field, an anisotropic and/or variable temperature distribution at the inner surface $r = r_i$, or inhomogeneities in the external medium. Here we will merely look at the effects on a static flow due to perturbations about its spherically symmetric solution.

For simplicity, we assume the energy density and pressure to be functions of temperature only, i.e. we use the equilibrium expression for the number density of electrons and positrons. As

we have seen, this is a good approximation inside the photosphere as far as the dynamics of the flow is concerned. Also, the flow is assumed to be azimuthally symmetric.

Defining the quantity $\sigma \equiv (\rho + P)/T$, the energy-momentum tensor can be written as

$$T^{\alpha\beta} = T\sigma U^\alpha U^\beta + Pg^{\alpha\beta}. \quad (105)$$

Contracting the equations of motion ($T^{\alpha\beta}_{;\beta} = 0$) with U_α results in the conservation law

$$(\sigma U^\mu)_{;\mu} = 0. \quad (106)$$

This can be used to simplify the equations of motion;

$$(g^{\alpha\beta} + U^\alpha U^\beta) T_{;\beta} + TU^\beta U^\alpha_{;\beta} = 0. \quad (107)$$

We now introduce the four-vector $V^\alpha = TU^\alpha$, which allows us to write equation (107) as

$$V^\alpha (V_{\alpha;\beta} - V_{\beta;\alpha}) \equiv V^\alpha \omega_{\alpha\beta} = 0. \quad (108)$$

We have here defined the vorticity tensor $\omega_{\alpha\beta} \equiv (TU_\alpha)_{;\beta} - (TU_\beta)_{;\alpha} = (TU_\alpha)_{;\beta} - (TU_\beta)_{;\alpha}$. It is straightforward to show that the circulation

$$\Gamma \equiv \oint TU_\alpha dx^\alpha = \int [(TU_\alpha)_{;\beta} - (TU_\beta)_{;\alpha}] dx^\alpha dx^\beta = \int \omega_{\alpha\beta} dx^\alpha dx^\beta \quad (109)$$

is unchanged along the path of a fluid element.

We are interested in axisymmetric ($\partial/\partial\phi = 0$) perturbations around spherically symmetric flow. Let the temperature of the unperturbed flow be $\bar{T}(r)$, and the nonzero components of the unperturbed four-velocity be $\bar{U}^0(r) = \bar{\gamma}(r)$ and $\bar{U}^r(r) = \bar{\gamma}(r)\bar{v}(r)$; consequently $\bar{V}^0(r) = \bar{T}(r)\bar{U}^0(r)$ and $\bar{V}^r(r) = \bar{T}(r)\bar{U}^r(r)$, and $\omega_{\alpha\beta} = 0$ for the unperturbed flow. Denote perturbed quantities by $\delta T(r, \theta)$, $\delta U^\mu(r, \theta)$ and $\delta V^\mu(r, \theta)$. From the fluid equations $V^\nu \omega_{\mu\nu} = 0$ we find, to first order in the perturbations,

$$\bar{V}^0 \omega_{\mu 0} + \bar{V}^r \omega_{\mu r} = 0. \quad (110)$$

The $\mu = 0$ and $\mu = r$ components of this equation both imply $\omega_{0r} = \partial\delta V_0/\partial r = 0$, so that $\delta V_0 = f(\theta)$, independent of r . Below, it will prove convenient to expand

$$f(\theta) = \frac{\bar{V}^0}{2} \sum_{\ell \neq 0} \ell(\ell + 1) \tau_\ell P_\ell(\theta), \quad (111)$$

where $P_\ell(\theta)$ is the Legendre function. We omit $\ell = 0$ in the sum because it may be absorbed into the background solution, for which $\bar{V}_0 = \text{constant}$. The $\mu = \theta$ component of equation (110) becomes

$$\omega_{\theta r} = \frac{\partial\delta V_\theta}{\partial r} - \frac{\partial\delta V_r}{\partial\theta} = \frac{\bar{V}^0}{\bar{V}^r} \frac{df(\theta)}{d\theta} = \frac{(\bar{V}^0)^2}{2\bar{V}^r} \sum_{\ell \neq 0} \ell(\ell + 1) \tau_\ell \frac{dP_\ell(\theta)}{d\theta} \quad (112)$$

after substituting for δV_0 . The $\mu = \phi$ component of equation (110) implies $\partial\delta V_\phi/\partial r = 0$, so that $\delta V_\phi = g(\theta)$, or $\sin^2\theta U^\phi = g(\theta)/\bar{T}(r)r^2$.

Next, we perturb the entropy equation, which may be written in the form

$$\frac{1}{r^2 \sin\theta} \frac{\partial(r^2 \sin\theta Q(T) V^\mu)}{\partial x^\mu} = 0, \quad (113)$$

where $Q(T) \equiv \sigma(T)/T$. To first order we find

$$\bar{V}^r \frac{\partial}{\partial r} \left(\nu(\bar{T}) \frac{\delta T}{\bar{T}} + \frac{\delta V^r}{\bar{V}^r} \right) + \frac{1}{r^2 \sin\theta} \frac{\partial(\sin\theta \delta V_\theta)}{\partial\theta} = 0 \quad (114)$$

where $\nu(T) \equiv d \ln Q(T)/d \ln T$, and $\delta V^\theta = g^{\theta\theta} \delta V_\theta = r^{-2} \delta V_\theta$.

The normalization condition $-T^2 = V^\mu V_\mu$ implies, to first order in the perturbations,

$$\bar{T} \delta T = -\bar{V}^0 f(\theta) - \bar{V}^r \delta V^r; \quad (115)$$

using this relationship to eliminate $\delta V^r = \delta V_r$ in equations (112) and (114) implies

$$\frac{\partial(\sin\theta \delta V_\theta)}{\partial r} + \frac{\bar{T}^2}{\bar{V}^r} \sin\theta \frac{\partial(\delta T/\bar{T})}{\partial\theta} = 0 \quad (116)$$

(where we have also multiplied by $\sin\theta$) and

$$\frac{\partial(\sin\theta \delta V_\theta)}{\partial\theta} + r^2 \sin\theta \bar{V}^r \frac{\partial[\nu_R(r)(\delta T/\bar{T})]}{\partial r} = \frac{2r \sin\theta f(\theta) \bar{T}^2 \bar{V}^0}{(\bar{V}^r)^3} \frac{d \ln \bar{T}}{d \ln r}, \quad (117)$$

where $\nu_R(r) \equiv \nu(\bar{T}) - (\bar{T}/\bar{V}^r)^2$. Differentiate equation (116) with respect to θ and equation (117) with respect to r to find

$$\frac{\bar{V}^r}{\bar{T}^2} \frac{\partial}{\partial r} \left[r^2 \bar{V}^r \frac{\partial}{\partial r} \left(\nu_R(r) \frac{\delta T}{\bar{T}} \right) \right] - \frac{1}{\sin\theta} \frac{\partial}{\partial\theta} \left[\sin\theta \frac{\partial}{\partial\theta} \left(\frac{\delta T}{\bar{T}} \right) \right] = \frac{2f(\theta)}{\bar{V}^0} \bar{H}(r), \quad (118)$$

where (recall that $d\bar{V}^0/dr = 0$)

$$\bar{H}(r) \equiv \frac{\bar{V}^r (\bar{V}^0)^2}{\bar{T}^2} \left[\frac{r \bar{T}^2}{(\bar{V}^r)^3} \frac{d \ln \bar{T}}{d \ln r} \right]_{,r}. \quad (119)$$

When the background flow is extremely relativistic and dominated by extremely relativistic particles, we may take $\bar{V}^r = \bar{V}^0$, $\bar{T} \propto 1/r$, and $\nu_R = 2$ up to corrections $\sim \bar{\gamma}^{-2}$. With these substitutions, $\bar{H}(r) = 1$ and equation (118) becomes

$$2\bar{\gamma}^2 \frac{\partial}{\partial r} \left[r^2 \frac{\partial}{\partial r} \left(\frac{\delta T}{\bar{T}} \right) \right] - \frac{1}{\sin\theta} \frac{\partial}{\partial\theta} \left[\sin\theta \frac{\partial}{\partial\theta} \left(\frac{\delta T}{\bar{T}} \right) \right] = \frac{2f(\theta)}{\bar{V}^0} = \sum_{\ell \neq 0} \ell(\ell+1) \tau_\ell P_\ell(\theta), \quad (120)$$

which has the general solutions

$$\frac{\delta T}{\bar{T}} = \sum_{\ell \neq 0} [\tau_\ell + c_\ell \cos(k_\ell/\bar{\gamma}(r)) + s_\ell \sin(k_\ell/\bar{\gamma}(r))] P_\ell(\theta), \quad (121)$$

where $k_\ell \equiv \sqrt{\ell(\ell+1)}/2$, and c_ℓ and s_ℓ are constants to be determined from boundary conditions. Notice that since $\bar{\gamma}(r) \propto r$, the temperature fluctuations become independent of r asymptotically:

$$\lim_{r \rightarrow \infty} \frac{\delta T}{\bar{T}} = \sum_{\ell \neq 0} (\tau_\ell + c_\ell) P_\ell(\theta). \quad (122)$$

From equations (121) and (116) we find

$$\delta V_\theta = \frac{r^2 \bar{T}^2}{\bar{V}^0} \sum_{\ell \neq 0} \left[\frac{\tau_\ell}{r} + \frac{c_\ell \bar{\gamma}}{k_\ell r} \sin(k_\ell/\bar{\gamma}(r)) - \frac{s_\ell \bar{\gamma}}{k_\ell r} \cos(k_\ell/\bar{\gamma}(r)) \right] \frac{dP_\ell(\theta)}{d\theta} + \frac{A_\theta}{\sin \theta}; \quad (123)$$

the additional solution proportional to $1/\sin \theta$ is a (singular) potential flow with no associated temperature perturbation. Since $\delta V_\theta = r^2 \bar{T} \delta U^\theta$, and $\bar{T}r = \text{constant}$, the non-radial velocity component $\delta v^\theta = r \delta U^\theta / \gamma \propto r^{-1}$ at large radii (ignoring the singular term in eq.[123]). From equation (115) we find that

$$\delta V_r = -\frac{\bar{V}^0}{2} \sum_{\ell \neq 0} \left\{ \tau_\ell \ell(\ell+1) + \frac{2\bar{T}^2}{(\bar{V}^0)^2} [c_\ell \cos(k_\ell/\bar{\gamma}(r)) + s_\ell \sin(k_\ell/\bar{\gamma}(r))] \right\} P_\ell(\theta); \quad (124)$$

here, we ignored a correction term $\propto \bar{T}^2/(\bar{V}^0)^2$ compared with $\ell(\ell+1)$ in the term $\propto \tau_\ell$. To leading order in $1/\bar{\gamma}^2$, $\delta V^r = \delta V^0$. We note that in this limit $\omega_{0\theta} = \omega_{\theta r} = df(\theta)/d\theta$. In the solutions given above, only the terms proportional to τ_ℓ represent flows with nonzero vorticity; the remaining terms are the general solution for perturbed potential flow.

Although memory of the temperature fluctuations at the inner boundary is maintained far out in the flow, it is the value of $V^0 = \gamma T$ that determines whether there are any observable consequences. As a result, if $f(\theta) = 0$, so that the flow is derivable from a potential, the radiation spectrum detected by a distant observer is the same as for the background spherical flow. If $f(\theta) \neq 0$, so that the flow has nonzero vorticity, distant observers detect a superposition of quasi-thermal spectra of the kind derived in Section 5.2. While these results have been derived for small axisymmetric perturbations about spherically symmetric flow, it is conceivable that when the perturbations become significant, the observed spectrum can appear substantially non-thermal.

6. Baryon Contamination and γ_∞

How is the $\dot{M} \rightarrow 0$ limit achieved for nonzero (baryon) mass ejection rate \dot{M} ? This question raises three subsidiary ones: (1) For a given \dot{E} , what is the critical value of \dot{E}/\dot{M} above which the flow is essentially the same as for $\dot{M} = 0$? (2) Since we know that the asymptotic Lorentz factor

γ_∞ is finite for $\dot{M} = 0$ (equation [71]), and that $\gamma_\infty \sim \dot{E}/\dot{M}$ for relatively large \dot{M} (small \dot{E}/\dot{M}), does γ_∞ grow monotonically with increasing \dot{E}/\dot{M} ? (3) What is the largest possible value of γ_∞ ?

Below, we demonstrate that $\gamma_\infty \sim \dot{E}/\dot{M}$ until it reaches a critical value

$$\left(\frac{\dot{E}}{\dot{M}}\right)_{c,M} \sim 350(Z/A)^{1/4}(r_i/10^6\text{cm})^{1/4}\gamma_i^{3/4}(T_i/m_e), \quad (125)$$

at which the radius $r_M \sim (\dot{E}/\dot{M})r_i$ where the flow becomes matter dominated first moves out to the photosphere. As \dot{M} decreases further, we find that γ_∞ remains virtually constant at $\sim (\dot{E}/\dot{M})_{c,M}$ until a second critical value

$$\left(\frac{\dot{E}}{\dot{M}}\right)_{c,P} \sim 7 \times 10^4(Z/A)(r_i/10^6\text{cm})(T_i/m_e), \quad (126)$$

above which the densities of electrons and positrons are nearly equal once pairs go out of equilibrium. Between $(\dot{E}/\dot{M})_{c,P}$ and

$$\left(\frac{\dot{E}}{\dot{M}}\right)_{c,0} \sim 5 \times 10^7(r_i/10^6\text{cm})(T_i/m_e) \quad (127)$$

the inertia in e^\pm pairs beyond the photosphere becomes progressively more important compared with the inertia in baryons, and γ_∞ grows from $\sim (\dot{E}/\dot{M})_{c,M}$ to roughly its maximum value, the $\dot{M} \rightarrow 0$ limit, which applies at $\dot{E}/\dot{M} \gtrsim (\dot{E}/\dot{M})_{c,0}$. Over the entire domain $\dot{E}/\dot{M} \gtrsim (\dot{E}/\dot{M})_{c,M}$, the value of γ_∞ only grows by a factor $\sim (Am_p/2Zm_e)^{1/4} \sim 10$.

6.1. Equilibrium flow

First, we review the results for an equilibrium flow with baryons (Paczynski 1986). From conservation of baryon number and energy, it follows that

$$\dot{N} \equiv 4\pi r^2 n \gamma v = \dot{M}/Am_p = \text{constant}; \quad (128)$$

$$\dot{E} \equiv 4\pi r^2 (\rho + P) \gamma^2 v = \text{constant}. \quad (129)$$

As before, we get $\gamma \propto r$ and $T \propto 1/r$ in a radiation dominated flow. This behavior is maintained until $\rho + p \sim nAm_p$, which occurs at a radius $r_M \approx (\dot{E}/\dot{M})(r_i/\gamma_i)$ where $\gamma \sim \dot{E}/\dot{M}$. In an equilibrium flow at sufficiently low T the optical depth is essentially $\tau \sim Zn\sigma_T r/\gamma$, resulting in

$$\tau \approx \frac{Z\dot{N}^4(Am_p)^3\gamma_i\sigma_T}{4\pi r_i\dot{E}^3} \times \begin{cases} (r_M/r)^3 & \text{for } r_M > r \\ (r_M/r) & \text{for } r_M < r. \end{cases} \quad (130)$$

A critical value of \dot{E}/\dot{M} is defined as the value which gives $\tau = 1$ at $r = r_M$, i.e. $r_{\text{ph}} = r_M$. With $\rho + P \sim (11/4)(4/3)(\pi^2/15)T_i^4$ at r_i , this gives

$$\left(\frac{\dot{E}}{\dot{M}}\right)_{c,M} \sim 350 \left(\frac{Z}{A}\right)^{1/4} \left(\frac{r_i}{10^6\text{cm}}\right)^{1/4} \gamma_i^{3/4} \frac{T_i}{m_e}. \quad (131)$$

The optical depth can then be rewritten as

$$\tau \approx \left[\frac{(\dot{E}/\dot{M})_{c,M}}{\dot{E}/\dot{M}} \right]^4 \times \begin{cases} (r_M/r)^3 & \text{for } r_M > r \\ (r_M/r) & \text{for } r_M < r. \end{cases} \quad (132)$$

If $\dot{E}/\dot{M} < (\dot{E}/\dot{M})_{c,M}$, r_M is inside the photosphere and we expect there to be little acceleration outside r_M , so the asymptotic Lorentz factor is \dot{E}/\dot{M} . If, on the other hand, $\dot{E}/\dot{M} > (\dot{E}/\dot{M})_{c,M}$, then r_M is outside the photospheric radius $r_{\text{ph}} \approx r_M \left[(\dot{E}/\dot{M})_{c,M} / (\dot{E}/\dot{M}) \right]^{4/3}$, and the Lorentz factor at r_{ph} is $\gamma_{\text{ph}} \approx \gamma_M(r_{\text{ph}}/r_M) \approx (\dot{E}/\dot{M})_{c,M}^{4/3} (\dot{E}/\dot{M})^{-1/3}$. The acceleration of the flow by the radiation flux beyond r_{ph} is found in a similar way as for the non-equilibrium pair wind, using

$$Am_p \frac{d\gamma}{dr} \approx Z\sigma_T F_0(r) = \frac{4\pi}{3} \left(\frac{r_{\text{ph}}\gamma_{\text{ph}}}{r\gamma} \right)^2 \sigma_T Z I_{\text{ph}} \left[1 - \left(\frac{r_{\text{ph}}\gamma}{r\gamma_{\text{ph}}} \right)^4 \right]. \quad (133)$$

For $r_M > r_{\text{ph}}$ this results in a final Lorentz factor $\gamma_\infty \sim (\dot{E}/\dot{M})_{c,M} < \dot{E}/\dot{M}$.

The use of a free streaming form for the radiation field for $\tau < 1$ implies that the radiative component of \dot{E} is constant in this regime. This is a good approximation when $\dot{E}/\dot{M} \gtrsim (\dot{E}/\dot{M})_{c,0}$ and the energy content of the baryons is negligible. When $\dot{E}/\dot{M} \lesssim (\dot{E}/\dot{M})_{c,M}$, the radiation energy is much smaller than the baryon energy outside the photosphere, and so the details of the radiation field are not dynamically important. In the intermediate regime, radiative acceleration increases the baryonic energy, causing a corresponding decrease in the radiative energy unaccounted for when using the free streaming approximation. The error thus made can be estimated as

$$\Delta \dot{E}_{\text{baryon}} / \dot{E} = (\gamma_\infty - \gamma_{\text{ph}}) \dot{M} / \dot{E} \sim \frac{(\dot{E}/\dot{M})_{c,M}}{\dot{E}/\dot{M}} \left\{ 1 - \left[\frac{(\dot{E}/\dot{M})_{c,M}}{\dot{E}/\dot{M}} \right]^{1/3} \right\}. \quad (134)$$

The maximum $\Delta \dot{E}_{\text{baryon}} / \dot{E}$ is ~ 0.1 and occurs at $\dot{E}/\dot{M} = (4/3)^3 (\dot{E}/\dot{M})_{c,M}$. Numerically we find the maximum gain in baryonic energy to be about 20 per cent of the total flow energy, with a functional dependence on \dot{E}/\dot{M} following roughly the estimate in equation (134). Since the error made in assuming a free streaming radiation field is relatively small as far as the dynamics is concerned and only affects a small interval in \dot{E}/\dot{M} , we adopted this simplification in our numerical calculations. The resulting values of γ_∞ are very accurate for \dot{E}/\dot{M} well above and well below $(\dot{E}/\dot{M})_{c,M}$, and should be correct to $\approx 10 - 20$ per cent for $\dot{E}/\dot{M} \sim (\dot{E}/\dot{M})_{c,M}$.

6.2. Baryons and non-equilibrium effects

With baryons in the flow, charge neutrality requires that the electron number density n_- , the positron number density n_+ , and the baryon number density n obey $n_- = n_+ + Zn$. The positron number density n_+ is then found from

$$\frac{1}{r^2} \frac{d}{dr} (r^2 n_+ \gamma v) = -\langle \sigma_{\text{ann}} v \rangle \left[(n_+ + Zn) n_+ - n_{\text{eq}}^2 \right], \quad (135)$$

where, as before, $n_{\text{eq}}^2 = (n_+ n_-)_{\text{eq}}$. At large \dot{M} , the excess of electrons over positrons is always large at $T < m_e$. The positron density first becomes important at r_{eq} when

$$\frac{\dot{E}}{\dot{M}} \sim \frac{Z m_e \gamma_i T_i}{A m_p m_e} \frac{C}{(\ln C)^4} \approx 3 \times 10^3 \frac{Z T_i}{A m_e} \left(\frac{r_i}{10^6 \text{cm}} \right) \quad (136)$$

where $C \equiv \pi(e^4/m_e^2)m_e^3 r_i/\gamma_i \approx 4.4 \times 10^{12} (r_i/10^6 \text{cm}) \gamma_i^{-1}$; positrons first become important at the photosphere and beyond when

$$\frac{\dot{E}}{\dot{M}} \approx \left(\frac{\dot{E}}{\dot{M}} \right)_{\text{c,P}} \approx \frac{Z m_e \gamma_i T_i}{A m_p m_e} \frac{C}{(\ln C)^3}. \quad (137)$$

For $\dot{E}/\dot{M} > (\dot{E}/\dot{M})_{\text{c,P}}$, the inertial mass density outside the photosphere is

$$\rho \approx A m_p n + 2 m_e n_+ \equiv n_+ m_{\text{eff}} \quad (138)$$

where the effective mass is approximately

$$m_{\text{eff}} \approx 2 m_e \left[1 + (\dot{M}/\dot{E})(T_i/m_e) C \gamma_i / 4 (\ln C)^3 \right], \quad (139)$$

which varies between $\approx A m_p / Z$ for $\dot{E}/\dot{M} \sim (\dot{E}/\dot{M})_{\text{c,P}}$ and $2 m_e$ for

$$\frac{\dot{E}}{\dot{M}} > \left(\frac{\dot{E}}{\dot{M}} \right)_{\text{c,0}} \approx \frac{T_i}{4 m_e} \frac{C \gamma_i}{(\ln C)^3}. \quad (140)$$

Notice that $(\dot{E}/\dot{M})_{\text{c,0}} \sim (A m_p / 2 Z m_e) (\dot{E}/\dot{M})_{\text{c,P}}$.

The acceleration caused by the radiation force for $\tau < 1$ can be estimated using

$$m_{\text{eff}} \frac{d\gamma}{dr} = \frac{4\pi}{3} \left(\frac{r_{\text{ph}} \gamma_{\text{ph}}}{r \gamma} \right)^2 \sigma_T I_{\text{ph}} \left[1 - \left(\frac{r_{\text{ph}} \gamma}{r \gamma_{\text{ph}}} \right)^4 \right], \quad (141)$$

resulting in

$$\gamma_{\infty} \sim \frac{(A m_p / 2 Z m_e)^{1/4} (\dot{E}/\dot{M})_{\text{c,M}}}{\left[1 + (\dot{M}/\dot{E})(T_i/m_e) C \gamma_i / 4 (\ln C)^3 \right]^{1/4}}. \quad (142)$$

Equation (142) shows that γ_{∞} rises slowly ($\sim [\dot{E}/\dot{M}]^{1/4}$) from $\sim (\dot{E}/\dot{M})_{\text{c,M}}$ at $\dot{E}/\dot{M} \sim (\dot{E}/\dot{M})_{\text{c,P}}$, to $\sim (A m_p / 2 Z m_e)^{1/4} (\dot{E}/\dot{M})_{\text{c,M}}$ at $\dot{E}/\dot{M} \gg (\dot{E}/\dot{M})_{\text{c,0}}$. Since $\gamma_{\infty} \sim (\dot{E}/\dot{M})_{\text{c,M}}$ for $(\dot{E}/\dot{M})_{\text{c,P}} \gtrsim \dot{E}/\dot{M} \gtrsim (\dot{E}/\dot{M})_{\text{c,M}}$, the total increase in γ_{∞} for *all* $\dot{E}/\dot{M} \gtrsim (\dot{E}/\dot{M})_{\text{c,M}}$ is a factor $\sim (A m_p / 2 Z m_e)^{1/4} \sim 6$. This alleviates any ‘fine-tuning’ problem necessary to produce large asymptotic Lorentz factors (although proportionality to T_i/m_e remains): Values within an order of magnitude of one another are found as long as \dot{E}/\dot{M} is sufficiently large.

This qualitative behavior is seen in the numerical solution: γ_{∞} is shown as a function of \dot{M}/\dot{E} in Fig. 9, clearly showing the four distinct regions discussed above. The transitions between the regions are seen to correspond to the critical points $(\dot{E}/\dot{M})_{\text{c,M}}$, $(\dot{E}/\dot{M})_{\text{c,P}}$, and $(\dot{E}/\dot{M})_{\text{c,0}}$, shown as dotted vertical lines in Fig. 9.

7. Discussion

In order to make our treatment of the relativistic $e^\pm\gamma$ wind somewhat more complete, we address briefly (and largely qualitatively) two additional questions: (1) What happens if the initial temperature is much higher than the electron mass, e.g. comparable to the mass of muons or even nucleons? (2) Do weak magnetic fields alter the flow significantly?

7.1. The effects of $T_i \gg m_e$

When $T \sim m_\mu$, the muons are in equilibrium with the radiation, $\mu^+ + \mu^- \leftrightarrow \gamma + \gamma$. As T drops below a few percent of m_μ , the muon pair annihilations freeze out in the same way as the electron–positron pair annihilations do at $T \sim 0.05m_e$. Going through the same calculations as for the electrons, we find that $r_{\text{eq},e}/r_{\text{eq},\mu} \sim m_\mu/m_e$, and that $\rho_\mu \approx \rho_e$ for $r > r_{\text{eq},e}$ assuming that the muons have not decayed before reaching $r_{\text{eq},\mu}$. (For $r_{\text{eq},\mu} \ll r \ll r_{\text{eq},e}$, $m_e \ll T \ll m_\mu$ and therefore $\rho_\mu \ll \rho_e$ in this regime.) However, the mean lifetime of a muon is only $t_\mu \sim 2.2 \times 10^{-6}$ seconds. They will therefore be significantly abundant at $r_{\text{eq},e}$ only if $t_\mu > \int_{r_{\text{eq},\mu}}^{r_{\text{eq},e}} dr/\gamma(r)$, i.e., if $\gamma_i > 80(r_i/10^6\text{cm})$. For γ_i smaller than this, the presence of muons in the flow will not have any significant influence on its dynamics. On the other hand, if γ_i is large enough for the muons to survive until γ reaches γ_∞ , then they will reduce the asymptotic Lorentz factor slightly because of their added contribution to the inertia of the flow. (Demanding $t_\mu > \int_{r_{\text{eq},\mu}}^{r_{\text{eq},e}} dr/\gamma(r)$ requires $\gamma_i > 1.9 \times 10^2[r_i/10^6\text{cm}]$.) For $T \ll m_e$, equation (26) reduces to

$$(\rho_e + \rho_\mu) \frac{d \ln \gamma}{d \ln r} \approx -\frac{r}{\gamma} G_0^r \approx \frac{r}{\gamma} 2n_e(\sigma_a + \sigma_s) F_0 \quad (143)$$

when muons are abundant. (Since $\sigma_T \propto m^{-2}$, we may neglect the muon contribution to the scattering cross section.) Thus the radiation force is approximately equal to that of a flow with only electrons and positrons, whereas the inertia is doubled since $\rho_e + \rho_\mu \approx 2\rho_e \approx 2m_e n_e$ in the region outside the photosphere. In the notation of Section 3.4, then, $\Lambda \rightarrow \Lambda/2$. And since $\gamma_\infty \sim \gamma_{\text{ph}} \Lambda^{1/4}$, the muons will reduce the asymptotic Lorentz factor by a factor $2^{1/4} \approx 1.2$, provided that most of them have not decayed by the end of the acceleration epoch. Ultimately, the relativistic muons decay, resulting in an additional non-thermal population of electrons.

In the arguments above we implicitly assumed that muons and electrons are coupled. Since their coupling via photons is very weak, the relevant remaining mechanism is through Coulomb scattering. The time-scale for Coulomb interaction is roughly (See e.g. Spitzer 1978)

$$t_c \sim \left\{ n_\mu \sqrt{\frac{T}{m_e}} \frac{e^4}{T^2} 4 \ln \left[(3/2e^3) \sqrt{T^3/\pi n_e} \right] \right\}^{-1}. \quad (144)$$

Comparing this to the expansion time-scale, $t_{\text{exp}} \sim r/\gamma$, we get $t_c/t_{\text{exp}} \sim 7.2 \times 10^{-5} (m_e/T)^{3/2}$, which is less than unity for $T/m_e > 1.7 \times 10^{-3}$. Recall that $T_{\text{ph}}/m_e \sim 0.037$ and $T_\gamma/m_e \sim 8 \times 10^{-4}$;

this indicates that the electrons and muons are marginally coupled for most of the acceleration regime $r_{\text{ph}} < r < r_\gamma$. The reduction of γ_∞ by a factor 1.2 therefore represents an estimate for the maximum change in the asymptotic Lorentz factor caused by the presence of muons in a flow with very high γ_i (or small r_i).

For high temperatures the inner portion of the wind can be optically thick to neutrinos as well. The cross section for electron–neutrino scattering is $\sigma_\nu \sim \sigma_0(T/m_e)^2$, where $\sigma_0 = 1.76 \times 10^{-44} \text{cm}^2$. The corresponding optical depth is

$$\tau_\nu(r) \sim \int_r^\infty dr n_e(r) \sigma_\nu(r) / \gamma(r) \sim 1.4 \times 10^{-8} \frac{1}{\gamma_i} \frac{r_i}{10^6 \text{cm}} \left(\frac{T}{m_e} \right)^5; \quad (145)$$

Consequently, $\tau_\nu > 1$ for $T/m_e > 37\gamma_i^{1/5}(r_i/10^6 \text{cm})^{-1/5}$. Neutrinos are kept in thermal equilibrium via reactions like $\nu_e + \bar{\nu}_e \leftrightarrow e^- + e^+$, whose rate exceeds the expansion rate for $T/m_e > 31\gamma_i^{1/5}(r_i/10^6 \text{cm})^{-1/5}$.

If T increases further we have to include not only muons in the flow, but also mesons. However, since mesons are very short-lived, their dynamical effect on the flow will be negligible. But for initial temperatures high enough for nucleon–anti-nucleon pairs to exist, there is the possibility that the surviving fraction (after annihilations freeze out) will result in a significant baryon loading in the wind. The cross section for nucleon–anti-nucleon annihilations is $\langle \sigma v \rangle \sim 1/m_\pi^2$, resulting in a freeze-out temperature of $T_{\text{eq,nucl}}/m_p \sim 0.026$. This results in negligible baryon loading in the wind: $\rho_{\text{nucl}}/\rho_{e^\pm} \sim 4 \times 10^{-6}$ for $r \gg r_{\text{eq,e}}$.

7.2. Effects of weak magnetic fields

In this subsection we will estimate how weak magnetic fields can affect the flow. The ‘background’ wind is assumed to expand radially, and we consider the effects of radial and tangential fields.

In Section 5.3 we presented a general treatment of perturbations of a flow with equation of state that depends only on temperature. When magnetic fields are present, and the electric field vanishes in the rest frame of the flow, the equation of entropy conservation, $(\sigma U^\mu)_{;\mu} = 0$ remains true, but the remaining fluid equations are modified to

$$V^\nu \omega_{\mu\nu} = \frac{F_{\mu\lambda} J^\lambda}{Q(T)} \quad (146)$$

where $F_{\mu\lambda}$ is the Maxwell tensor, and J^λ is the current density four vector.

We can use equation (146) to examine the effects on the flow of a magnetic field; to do so requires solving Maxwell’s equations simultaneously. A particularly simple example is a radially directed magnetic field, as might arise, for example, if the flow originates on a magnetized star, and pulls magnetic field lines outward along with it. In that case, it is easy to show that, assuming

axisymmetry, the magnetic field strength is proportional to $b(\theta)/r^2$, where $b(\theta)$ is arbitrary. To lowest order, the electric field associated with a radial magnetic field vanishes in the frame of a stationary observer as well as in the frame comoving with the flow.

Under such conditions, the magnetic field engenders *no* change in γT to first order. This follows from the $\mu = r$ component of equation (146), which implies $\overline{V}^0 \omega_{0r} = 0$, or $\partial \delta V_0 / \partial r = 0$. (A similar conclusion follows from the $\mu = 0$ component of eq. [146].) Thus, the only perturbations to δV_0 are those imposed at the inner radius of the flow, as discussed in Section 5.3; none are created by the field. Radial magnetic fields drive non-radial flows whose amplitudes decline with radius even outside the photosphere (Grimsrud 1998).

Changes in γT require a non-radial magnetic field. The condition of perfect conductivity, $\mathbf{E} + \mathbf{v} \times \mathbf{B} = 0$, and Faraday's law imply $\mathbf{E} = -\nabla\psi = -\mathbf{v} \times \mathbf{B}$ in steady state; for axisymmetry we find, to lowest order,

$$\mathbf{B} = -\frac{\hat{\mathbf{e}}_\phi}{rv(r)} \frac{d\psi(\theta)}{d\theta} \quad \mathbf{E} = -\frac{\hat{\mathbf{e}}_\theta}{r} \frac{d\psi(\theta)}{d\theta}. \quad (147)$$

Associated with ordered tangential fields is a Poynting flux in the stationary frame,

$$\mathbf{S} = \frac{\hat{\mathbf{e}}_r}{4\pi r^2 v(r)} \left(\frac{d\psi(\theta)}{d\theta} \right)^2; \quad (148)$$

there is no Poynting flux for radially directed \mathbf{B} to lowest order (since $\mathbf{E} = 0$), and there is, of course, no Poynting flux in the comoving frame. Note that $4\pi r^2 \mathbf{S}$ decreases with increasing radius as $v(r) \rightarrow 1$ from below. For these fields the $\mu = 0$ component of equation (146) implies

$$\frac{\partial \delta V_0}{\partial r} = \frac{1}{4\pi r^2 Q(\overline{T}) \overline{V}^r} \left(\frac{d\psi(\theta)}{d\theta} \right)^2 \frac{d}{dr} \left(\frac{1}{v} \right) = -\frac{1}{4\pi r^2 Q(\overline{T}) \overline{V}^r v^3 \overline{\gamma}^3} \left(\frac{d\psi(\theta)}{d\theta} \right)^2 \frac{d\overline{\gamma}}{dr}; \quad (149)$$

the $\mu = r$ component of equation (146) yields an identical result. In the extreme relativistic limit, where $\overline{\gamma} \propto r$ and $Q(\overline{T}) \propto \overline{T}^2 \propto r^{-2}$, equation (149) has the solution

$$\delta V_0 = \frac{1}{8\pi r^2 Q(\overline{T}) \overline{\gamma}^2 \overline{V}^0} \left(\frac{d\psi(\theta)}{d\theta} \right)^2 = \frac{|\mathbf{B}|^2}{8\pi Q(\overline{T}) \overline{\gamma}^2 \overline{V}^0}, \quad (150)$$

so $\delta V_0 \propto r^{-2}$. Although tangential fields alter γT , the perturbation peaks near the lift-off radius, and decreases far out in the flow. We therefore expect little or no effect on the observed radiation spectrum as a consequence of such fields. There is additional radial acceleration of the e^\pm pairs outside the photosphere as a consequence of the tangential field; we estimate the change in bulk Lorentz factor of the pairs to be $\Delta\gamma \approx (d\psi(\theta)/d\theta)^2 / 4m_e \dot{N}_{ph} \gamma_{ph}^2$ if pair annihilation can be neglected outside the photosphere, so the pair loss rate \dot{N} becomes independent of radius.

8. Conclusions

Radiation energy can escape from a fireball in two different ways: If there is significant baryon contamination present, much of the energy will be converted into bulk kinetic energy (Shemi & Piran 1990). However, when the expanding atmosphere has swept up a significant amount of surrounding matter, kinetic energy can be converted into escaping radiation at the resulting shock front (Mészáros & Rees 1993). In a similar way, internal shocks due to a non-uniform velocity can convert kinetic energy into radiation (Rees & Mészáros 1994). The other mechanism for radiation escape is more direct: If the particle content is small, the fireball can become optically thin before being matter dominated.

In this paper we have considered an extreme case of the latter possibility, in which there are no baryons present. The opacity is then due to electron–positron pairs, resulting in a very large optical depth for temperatures greater than the electron mass. Further out in the flow the temperature decreases, pair creation is suppressed and annihilations freeze in; this results in a small but non-negligible amount of surviving pairs. The radiation force acting on the particles accelerates the pairs considerably, even after the flow has become optically thin. We found that the Lorentz factor of the flow approaches the constant value $\gamma_\infty \sim 1.4 \times 10^3 \gamma_i^{3/4} (T_i/m_e)[(\sigma_a/\sigma_T) + (\sigma_s/\sigma_T)]^{1/4}$ only when the optical depth falls below $\tau_\gamma \sim 1.7 \times 10^{-5} \gamma_i^{3/4}$. This increases the asymptotic energy content of the pairs by a large factor, their fraction of the total energy approaching $\sim 8.5 \times 10^{-6} \gamma_i^{3/4} [(\sigma_a/\sigma_T) + (\sigma_s/\sigma_T)]^{1/4}$. The flow is always radiation dominated for reasonable values of the input parameters.

Even if the initial temperature were much higher than the electron mass, the resulting flow would not deviate significantly from an $e^\pm\gamma$ wind. If there are muons present, they will decay before the electron–positron annihilations freeze out, unless γ_i is very large. And even for γ_i high enough for the muons to survive until far outside the photosphere, their added inertia will only reduce the asymptotic Lorentz factor by at most 20 per cent. For even higher T_i , one may have nucleon–anti-nucleon pairs present in the flow. However, nucleon–anti-nucleon annihilations freeze out at a relatively low temperature, thus causing the baryon contamination in the flow to be negligible.

The photon distribution function in the comoving frame is very close to that of blackbody radiation. This is because $\gamma \propto r$ and $\gamma T \approx \text{constant}$ are excellent approximations in the flow until $r = r_\gamma$ where the optical depth is $\tau_\gamma \sim 1.7 \times 10^{-5} \gamma_i^{3/4}$. Practically all the observed radiation therefore originates from a region where these two approximations hold. As was discussed in Section 5, the conditions $\gamma \propto r$ and $\gamma T = \text{constant}$ imply that the equation of radiative transfer is solved by a blackbody distribution function in the comoving frame of the flow. The spectrum seen by an observer in the lab frame will deviate somewhat from a blackbody in that it has a broader peak and a shallower slope at low photon energies. Such spectra are *not* typical of observed γ –ray bursts, which are characterized by flat fluxes for logarithmic energy intervals (e.g. Schaefer et al. 1992, 1994; Kouveliotou 1994). A superposition of quasi-thermal spectra from numerous

source regions radiating independently (but with different physical parameters) might produce flat spectra. The non-radial perturbation calculations discussed in Section 5.3 lend partial support to this idea.

Ordered magnetic fields (whose energy content is small compared to that of the flow) will make the temperature and the velocity of the flow anisotropic and may enhance the bulk Lorentz factor of e^\pm pairs beyond the photosphere, but do not affect the spectrum seen by a distant observer significantly.

The results obtained for zero baryon number also apply when the baryon loading is sufficiently small. For very large baryon loading, the flow becomes matter dominated at optical depths larger than one, and in this case the asymptotic Lorentz factor $\gamma_\infty \sim \dot{E}/\dot{M}$. As \dot{E}/\dot{M} increases above $(\dot{E}/\dot{M})_{c,M} \sim 350(Z/A)^{1/4}(r_i/10^6\text{cm})^{1/4}\gamma_i^{3/4}T_i/m_e$, the asymptotic Lorentz factor at first levels off at $\gamma_\infty \sim (\dot{E}/\dot{M})_{c,M}$. For still larger $\dot{E}/\dot{M} \gtrsim (\dot{E}/\dot{M})_{c,P} \sim 7 \times 10^4(Z/A)(r_i/10^6\text{cm})(T_i/m_e)$, the asymptotic Lorentz factor rises $\sim (\dot{E}/\dot{M})^{1/4}$, until $\dot{E}/\dot{M} \sim (\dot{E}/\dot{M})_{c,0} \sim (Am_p/2Zm_e)(\dot{E}/\dot{M})_{c,P}$. The $\dot{M} \rightarrow 0$ limit applies for $\dot{E}/\dot{M} > (\dot{E}/\dot{M})_{c,0} \sim 5 \times 10^7(r_i/10^6\text{cm})(T_i/m_e)$; in this regime, $\gamma_\infty \sim (Am_p/2Zm_e)^{1/4}(\dot{E}/\dot{M})_{c,M}$. The fraction of the total wind luminosity that emerges in the form of bulk kinetic energy falls below one at $\dot{E}/\dot{M} \sim (\dot{E}/\dot{M})_{c,M}$, and decreases monotonically until asymptoting to a finite value $\sim 10^{-5}\gamma_i^{3/4}$ as $\dot{M} \rightarrow 0$ (see equation [75]). Thus, for all $\dot{E}/\dot{M} > (\dot{E}/\dot{M})_{c,M}$, the asymptotic Lorentz factor varies by a factor of only $\sim (Am_p/2Zm_e)^{1/4} \sim 6$. The maximum possible γ_∞ is the value found for $\dot{M} = 0$ and is finite. Although we have only considered steady winds here, it seems likely that similar results would hold for fireballs originated impulsively.

This research was supported in part by NSF grant AST 93-15375 and NASA grant NAG 5-3097. OMG thanks Nansenfondet for financial support.

REFERENCES

- Abramowicz M. A., Novikov I. D., Paczyński B., 1991, ApJ, 369, 175
 Fenimore E. E., 1997, in Olinto A., Friemann J., Schramm D., eds, Proc. 18th Texas Symposium on Relativistic Astrophysics
 Fuller G. M., Shi X., 1997, astro-ph/9711020
 Goodman J., Dar A., Nussinov S., 1987, ApJ, 314, L7
 Grimsrud O. M., 1998, PhD thesis, Cornell University
 Hummer D. G., Rybicki G. B., 1971, MNRAS, 152, 1
 Kobayashi S., Piran T., Sari R., 1997, ApJ, 490, 92
 Kouveliotou C., 1994, ApJS, 92, 637

- Lee B. W., Weinberg S., 1977, *Phys. Rev. Lett.*, 39, 165
- Mészáros P., Rees M. J., 1993, *ApJ*, 405, 278
- Mihalas D., Mihalas B. W., 1984, *Foundations of Radiation Hydrodynamics*. Oxford Univ. Press, Oxford
- Naryan R., Paczyński B., Piran T., 1992, *ApJ*, 395, L83
- Paczyński B., 1986, *ApJ*, 308, L43
- Paczyński B., 1990, *ApJ*, 363, 218
- Paczyński B., 1997, *astro-ph/9712123*
- Pen U., Loeb A., Turok N., 1997, *astro-ph/9712178*
- Piran T., 1997, in Bahcall J., Ostriker J.P., eds, *Unsolved Problems in Astrophysics*. Princeton Univ. Press, Princeton
- Rees M. J., Mészáros P., 1992, *MNRAS*, 258, L41
- Rees M. J., Mészáros P., 1994, *ApJ*, 430, L93
- Rybicki G. B., Lightman A. P., 1979, *Radiative Processes in Astrophysics*. John Wiley & Sons, New York
- Schaefer B. E. et al., 1992, *ApJ*, 393, L51
- Schaefer B. E. et al., 1994, *ApJS*, 92, 285
- Shemi A., Piran T., 1990, *ApJ*, 365, L55
- Spitzer L., 1978, *Physical Processes in the Interstellar Medium*. John Wiley & Sons, New York
- Svensson R., 1982, *ApJ*, 258, 321
- Waxman E., 1997, *ApJ*, 485, L5
- Waxman E., Kulkarni S. R., Frail D. A., 1998, *ApJ*, 497, 288
- Wijers R., Rees M. J., Mészáros P., 1997, *MNRAS* 288, L51
- Weinberg S., 1972, *Gravitation and Cosmology*. John Wiley & Sons, New York

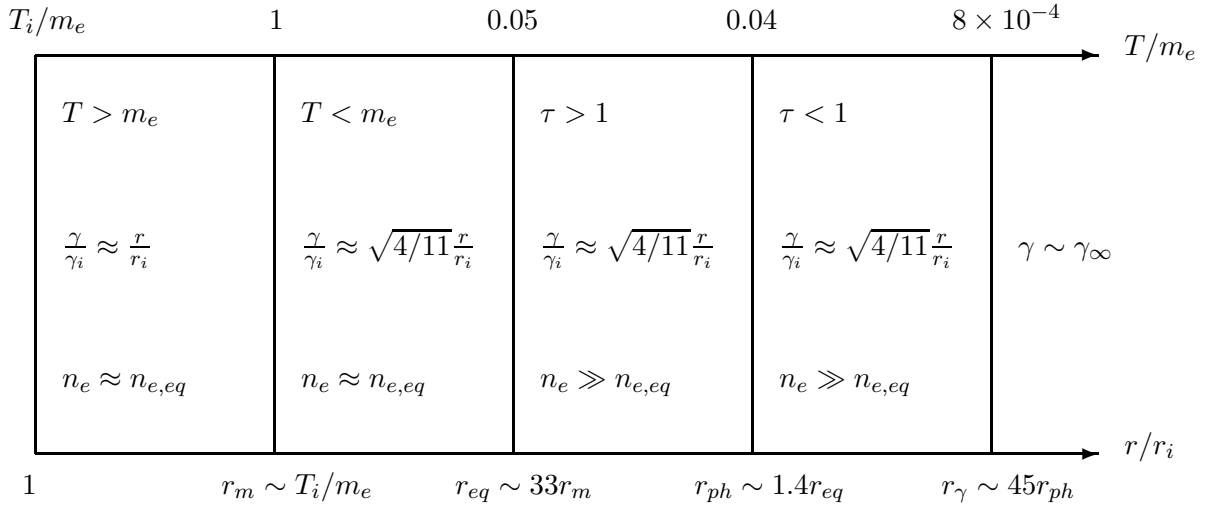


Fig. 1.— Summary of analytical model with γ_i and $r_i/10^6$ cm both of order unity.

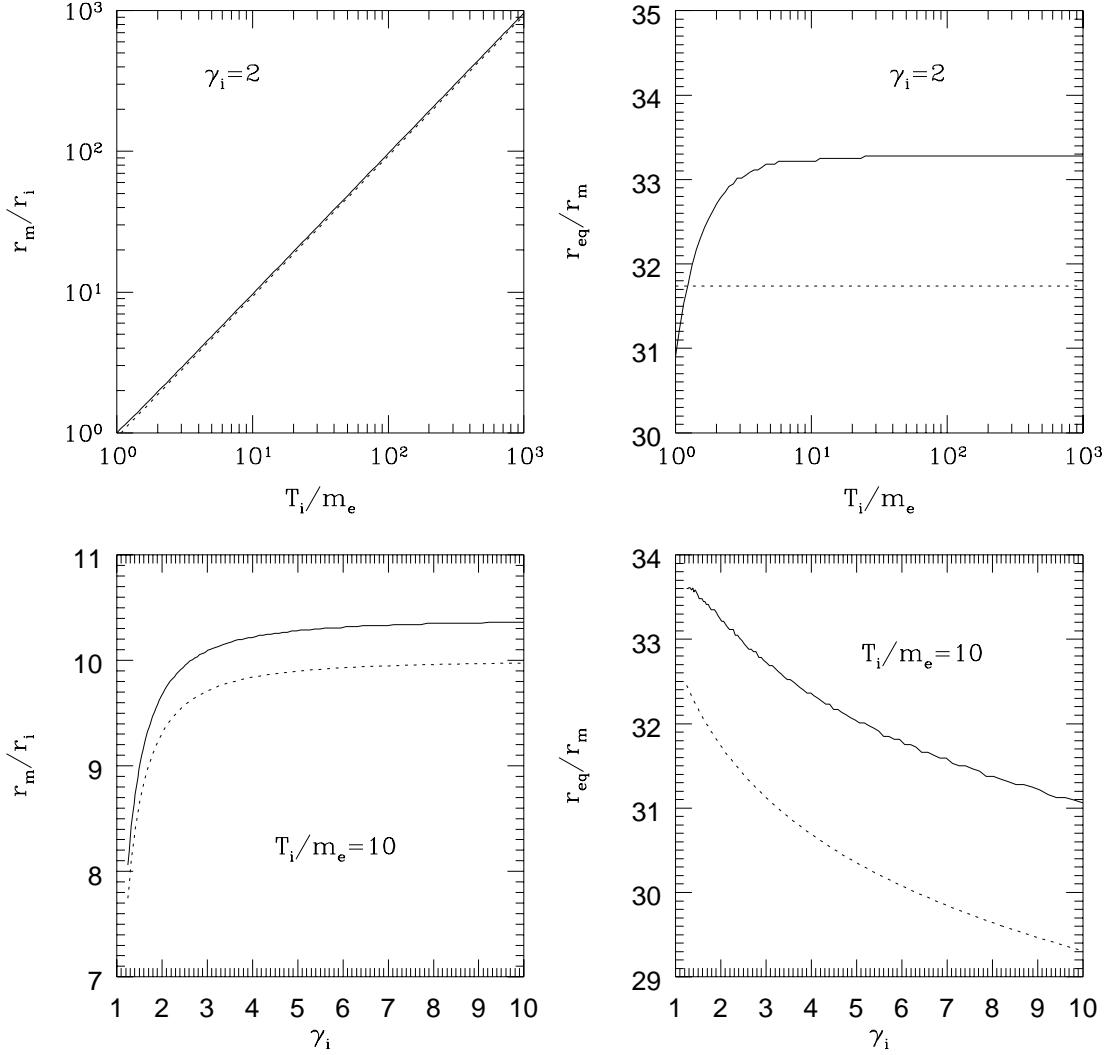


Fig. 2.— The ratios r_m/r_i and r_{eq}/r_m are shown as functions of the initial temperature T_i for fixed initial Lorentz factor γ_i in the upper panels, and as a function of γ_i for fixed T_i in the lower panels. r_i is the initial radius, $r_m \equiv r(T = m_e)$ and $r_{eq} \equiv r(n_e = 2n_{e,eq})$. The absorption cross section is $\sigma_a = 10^{-3}\sigma_T$. The solid lines correspond to the numerical solution, and the dotted lines to the analytical model.

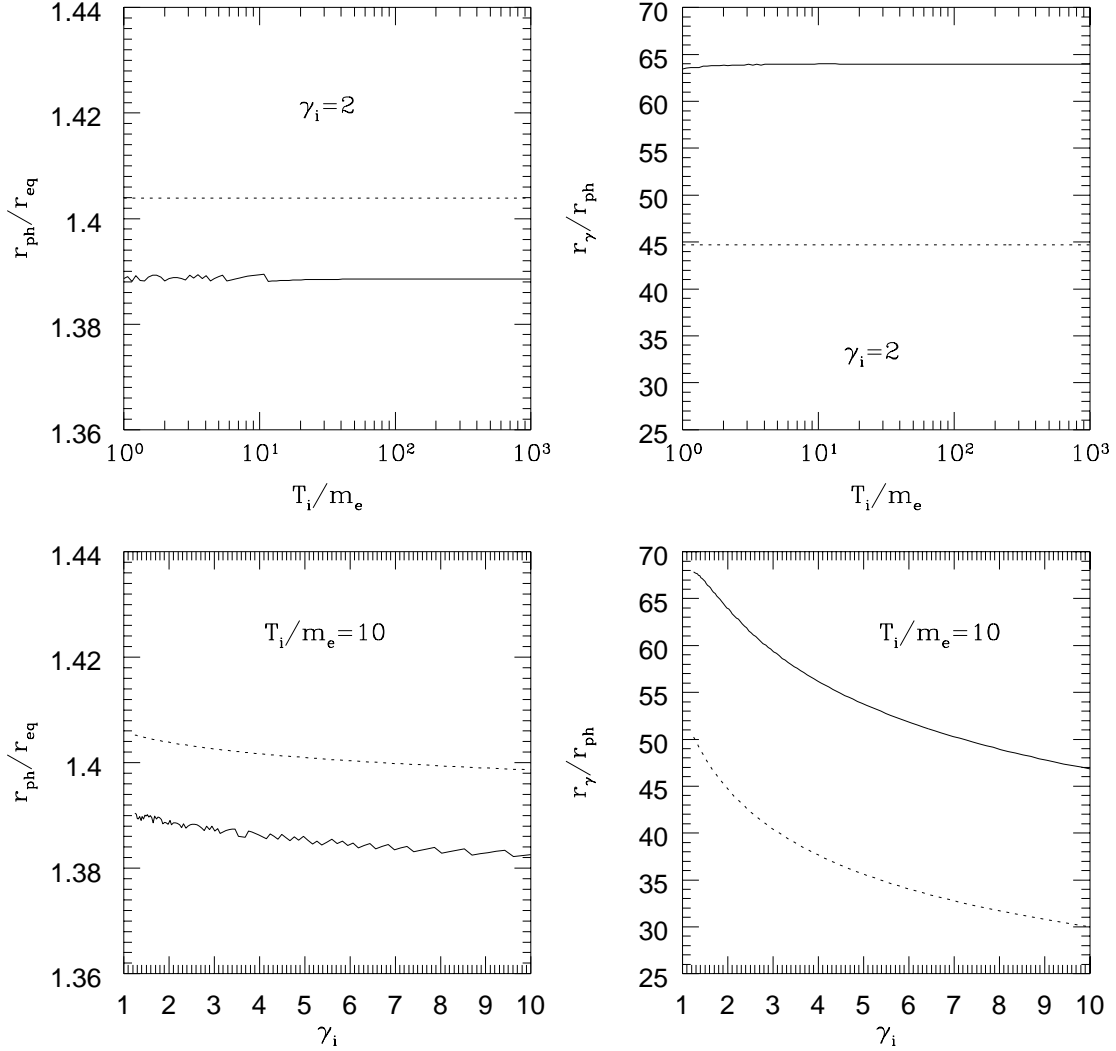


Fig. 3.— The ratios $r_{\text{ph}}/r_{\text{eq}}$ and r_{γ}/r_{ph} are shown as functions of initial temperature T_i and initial Lorentz factor γ_i . $r_{\text{eq}} \equiv r(n_e = 2n_{e,\text{eq}})$, $r_{\text{ph}} \equiv r(\tau = 1)$ and $r_{\gamma} \equiv r(\zeta = 1/2)$. The absorption cross-section is fixed at $\sigma_a = 10^{-3}\sigma_T$. The solid lines correspond to the numerical solution, and the dotted lines to the analytical model.

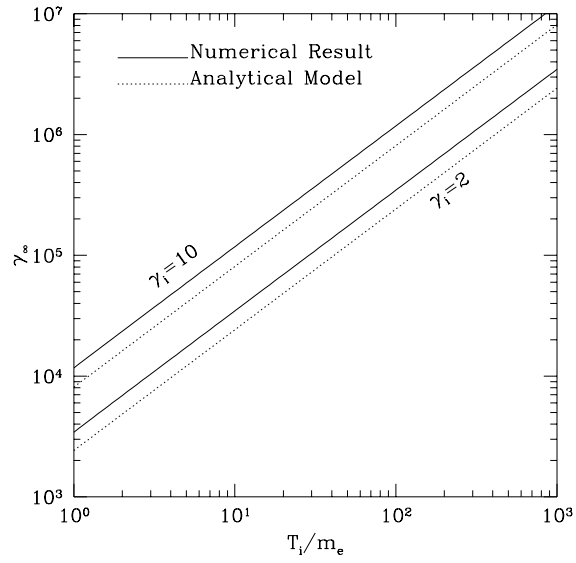


Fig. 4.— The asymptotic Lorentz factor as a function of the initial temperature for $\gamma_i = 2$ and $\gamma_i = 10$. The absorption cross-section is held fixed at $\sigma_a = 10^{-3}\sigma_T$.

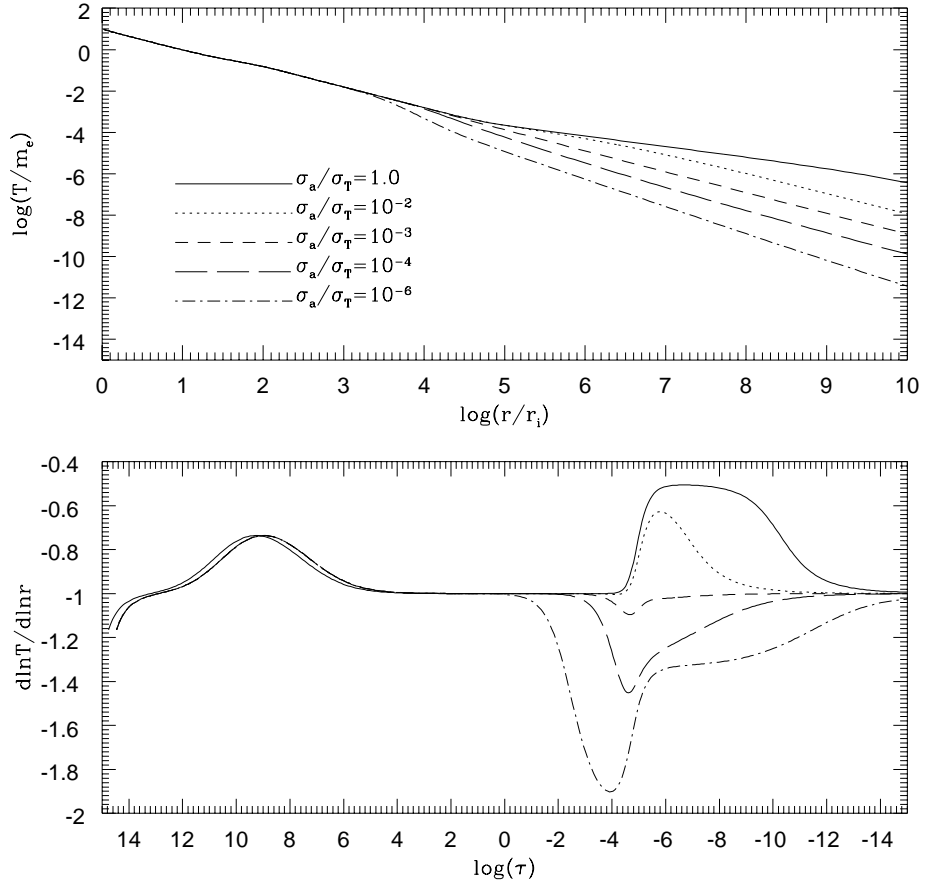


Fig. 5.— The local temperature $T(r)$ in units of m_e , and its derivative $d \ln T / d \ln r(\tau)$, are plotted for different absorption cross-sections. In these plots, $T_i = 10m_e$ and $\gamma_i = 2$.

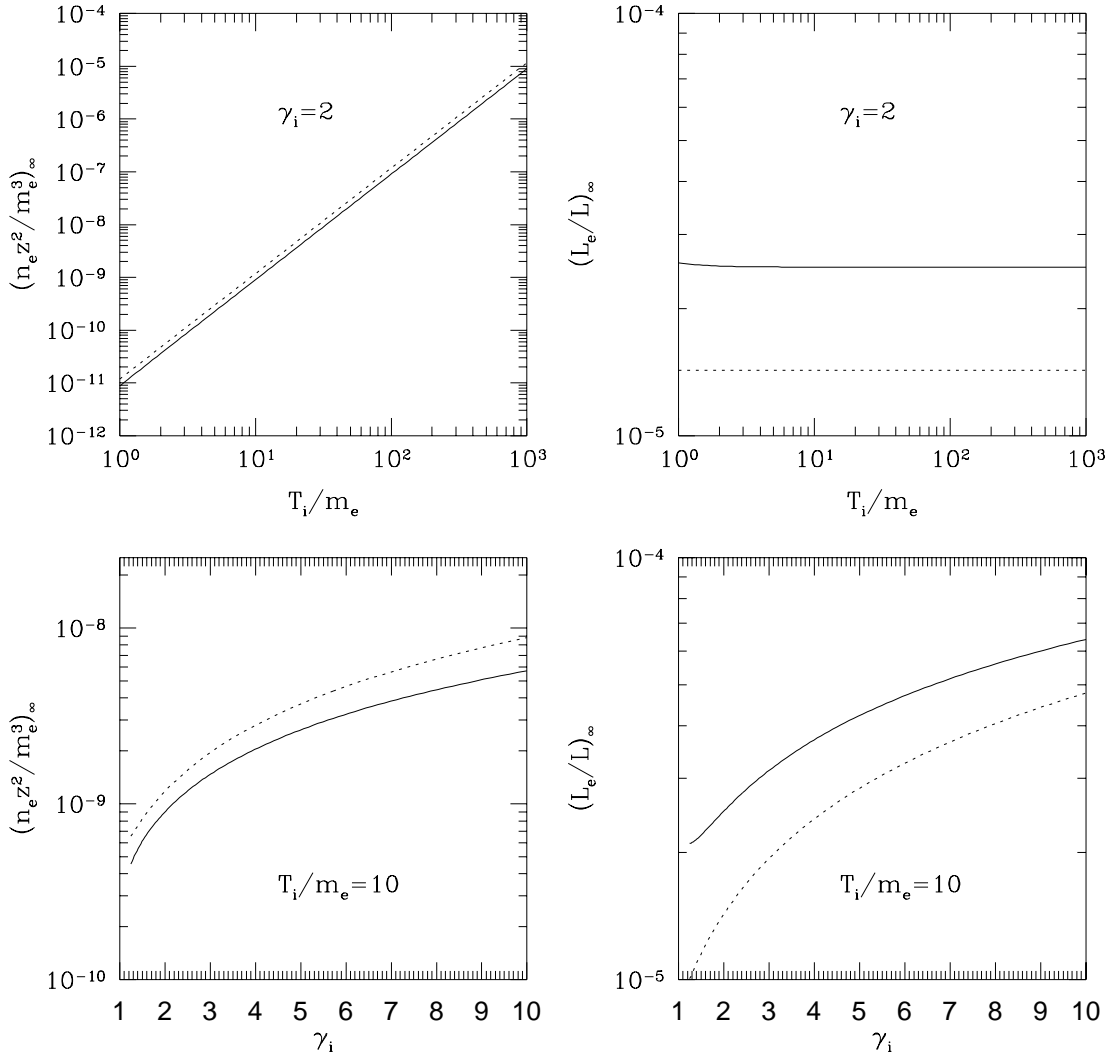


Fig. 6.— The asymptotic pair number density n_e times $z^2 = (r/r_i)^2$ is shown in the left panels in units of m_e^3 as a function of initial temperature T_i and Lorentz factor γ_i . The right panels show the asymptotic energy content in the pairs relative to that in the radiation. In all plots, $\sigma_a = 10^{-3}\sigma_T$. Solid lines represent the numerical solution and dotted lines the analytical model.

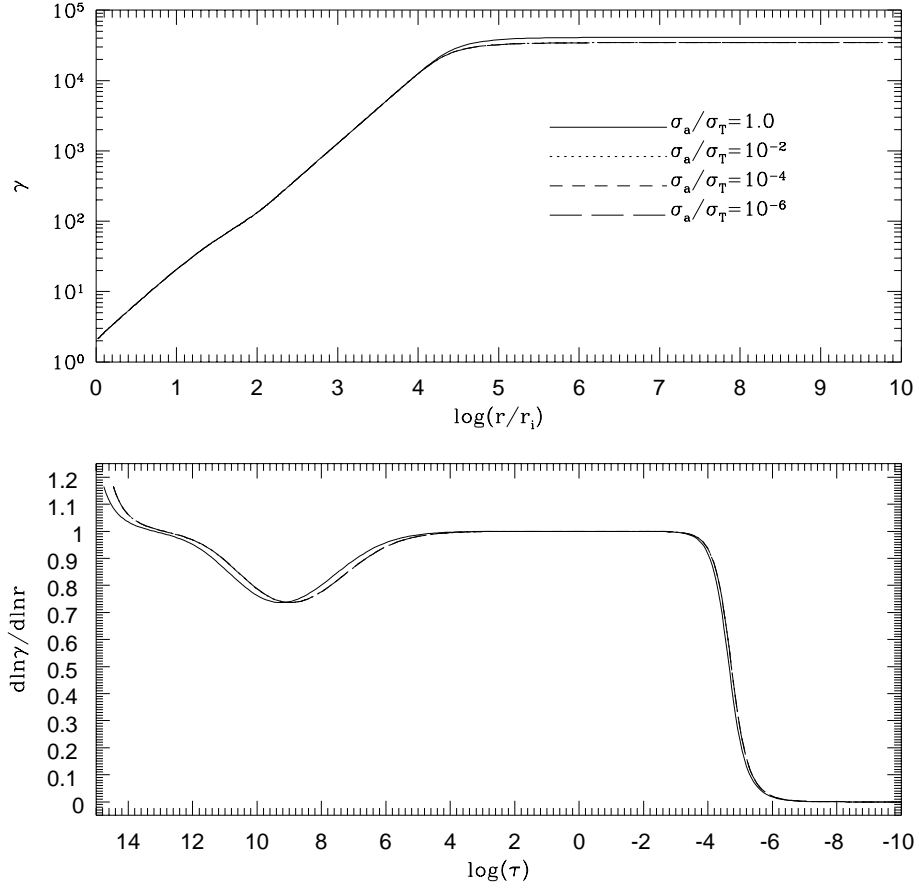


Fig. 7.— The Lorentz factor $\gamma(r)$ and its derivative $d \ln \gamma / d \ln r(\tau)$ are shown for a set of different absorption cross-sections. $T_i = 10m_e$ and $\gamma_i = 2$ are fixed.

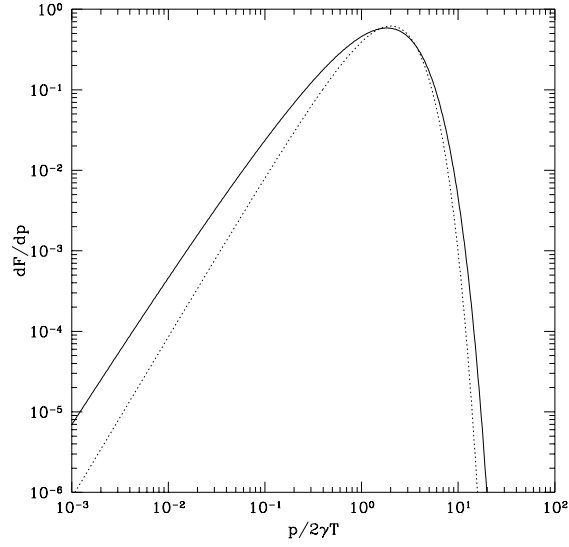


Fig. 8.— The spectrum seen by an observer in the lab frame (solid line) compared to blackbody (dotted line). The units for the flux are arbitrary.

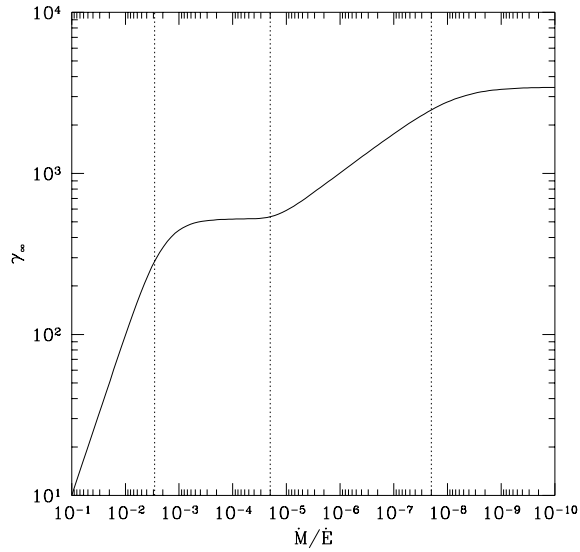


Fig. 9.— Asymptotic Lorentz factor as a function of \dot{M}/\dot{E} , the ratio of the mass injection rate to the energy injection rate. The dotted vertical lines correspond to the transition points $(\dot{E}/\dot{M})_{c,M}$, $(\dot{E}/\dot{M})_{c,P}$, and $(\dot{E}/\dot{M})_{c,0}$. In this example, $T_i/m_e = 1$, $\gamma_i = 2$, $\sigma_a/\sigma_T = 10^{-3}$, $\sigma_s/\sigma_T = 1$ and $A = Z = 1$.